Bio-electrochemical activity of *Clostridium ljungdahlii* at different electric potentials

Master's thesis

Author: Fahim Hadi

Supervisor: Chaeho Im

August 2021

CHALMERS

Abstract

Humans are responsible for a large portion of the emissions of CO_2 gas since the industrial revolution. The levels of emissions must decrease so that the increase of temperature should not exceed an increase of 2 °C by the end of this century. CO_2 fermentation is a promising technology that could reduce the amount of CO_2 in the atmosphere. *Clostridium ljungdahlii* is an interesting anaerobic microorganism capable of fermenting CO_2 and produce valuable chemicals such as ethanol. *C. ljungdahlii* is also capable of accepting electrons from an electrode in a bio-electrochemical system. The bio-electrochemical activity of *C. ljungdahlii* was thus investigated at the electric potentials -400, -600, -800 and -1000 mV. This was done by running biotic and abiotic bio-electrochemical system experiments at the mentioned potentials, as well as serum flask control experiments. The results were analysed in terms of product formation, growth, pH, current consumption, and redox species present in the bio-electrochemical system reactors. *C. ljungdahlii* showed no growth in the optical density measurements, but it could be seen that 2,3-butanediol was produced at -800 mV. Furthermore, calculations of coulombic efficiencies showed that the current consumption was very low.

Table of contents

1. Introduction

Humans are responsible for 47 % of the elevation of CO_2 levels since the industrial revolution and the levels in the air are at their highest levels in 650,000 years (NASA, 2021a). Two-thirds of the contribution to the heating imbalance that causes the temperature rise is due to the increase of CO_2 in the atmosphere (NOAA, 2021). According to the Paris agreement, the increase of temperature should not exceed an increase of 2 °C by the end of this century (UNFCCC, 2021). The average global temperature has increased with 1.1 °C since the year of 1880, the amount of arctic ice is decreasing by 13.1 percent per decade, and we are losing 427 billion tons of ice sheets per year (NASA, 2021b). CO_2 is what is called a greenhouse gas since it goes up to the atmosphere and contributes to trap heat in our planet (NOAA, 2021). There is thus a need for reducing the CO_2 emissions and the human impact on the greenhouse effect. Two ways of achieving this is by using alternatives that include biofuels and syngas.

1.1 Biofuels and syngas

One way to reduce CO_2 emissions is by using biofuels instead of fossil fuels. Biofuels are any fuel that is derived from replenishable biomass such as plants, algae, or animal waste (Britannica, 2021). Life cycle assessments have shown that the amount of emitted CO_2 to the atmosphere is much smaller by choosing biofuels rather than conventional fuels (Lin & Lu, 2021). Lignocellulosic biomass is an example of a feedstock that is used for producing biofuels (Liew et al., 2016; Lin & Lu, 2021; Sun et al., 2019). The lignocellulosic biomass can be hydrolysed by enzymes (Choudhary et al., 2020) but this requires many pre-treatment and hydrolysis steps since the lignin must be separated from the useful cellulose and hemicellulose (Liew et al., 2016; Sun et al., 2019). The latter must then be broken down to poly- and monosaccharides (Liew et al., 2016). This process is expensive and uses a lot of water (Liew et al., 2016). Furthermore, the lignin which can amount up to 40 percent of the biomass, cannot be used (Liew et al., 2016).

If the biomass instead would be combusted for syngas production, the many steps could be avoided and thus making it less expensive (Liew et al., 2016; Sun et al., 2019). The combustion can be done by letting the biomass react with steam and air at temperatures between 600-1000°C and pressures above 30 bar (Liew et al., 2016). Syngas can also be produced by combusting for municipal solid waste, organic industrial waste, or taken directly from off-gases from steel mills (Liew et al., 2016; Sun et al., 2019). Syngas itself contains mainly CO, H_2 and CO_2 but also for example, methane, ethane, nitrogen oxides, NH_3 and HCN (Liew et al., 2016; Sun et al., 2019). The content of the syngas can vary depending on several variables such as the feedstock, the temperature, the type of oven used or the oxidizing agent during combustion (Liew et al., 2016; Sun et al., 2019).

One way of converting syngas into high value chemicals is using the Fischer-Tropsch process (Liew et al., 2016; Sun et al., 2019). The Fischer-Tropsch process uses metal catalysts such as cobalt, ruthenium and iron and require high temperatures and high pressures, between 150-300° C and up to 30 bar (Liew et al., 2016). The Fischer-Tropsch process requires specific H_2:CO ratios that are higher than what normally is found in syngas and the catalyst is easily

poisoned by other gases (Liew et al., 2016; Sun et al., 2019). If not using the Fischer-Tropsch process, the gas can be fermented with microorganisms. Then ambient temperature and atmospheric pressure is needed (Liew et al., 2016; Sun et al., 2019). Also, the conversion efficiency is much higher while having higher product selectivity (Liew et al., 2016).

1.2 Acetogens

The microorganisms of interest in this report belong to what is called acetogens. Acetogens is the name for a mixed group of bacteria that produce acetyl-CoA via the Wood-Ljungdahl pathway (Schuchmann & Müller, 2016). Autotrophic acetogen produce acetyl-CoA from two molecules of CO_2 (Schuchmann & Müller, 2016) and they are responsible for fixing one fifth of the CO_2 on earth (Marcellin et al., 2016). Acetogens are strict anaerobes (Schuchmann & Müller, 2016) and have been found in about 20 different genera and more than 100 species have been discovered (Liew et al., 2016). Acetogens can be found in many different environments such as the human intestine, soil, and waste waters (Schuchmann & Müller, 2014; Sun et al., 2019). The most known acetogens belong the genera *Clostridium* and *Acetobacterium* and examples of two well-studied species are *Clostridium ljungdahlii* and *Acetobacterium woodii* (Schuchmann & Müller, 2014). The main product of acetogens is acetate but chemicals such as ethanol and butanol can also be produced (Sun et al., 2019).

1.2.1 The Wood-Ljungdahl pathway

The Wood-Ljungdahl pathway is known as one of the oldest biochemical pathways that enables biomass production from CO_2 and CO (Schuchmann & Müller, 2014). It can be found in many organisms but in this report, it will be focused on the one found in *C. ljungdahlii*. *C. ljungdahlii* can use CO or CO_2 with H_2 as input for the Wood-Ljungdahl pathway, but the focus will lay on the use of CO_2 and H_2 as input. Throughout the pathway 2 molecules of CO_2 and 1 ATP is consumed to produce acetyl-CoA (Liew et al., 2016; Schuchmann & Müller, 2014). 1 ATP is then produced if acetate is produced from acetyl-CoA. The reducing equivalents in the Wood-Ljungdahl pathway represented as electrons in figure 1 are H_2, reduced ferredoxin, NADH and NADPH (Schuchmann & Müller, 2014).

The Wood-Ljungdahl pathway consists of two different branches. The methyl branch where the end-product is a methyl-tetrahydrofolate, and the carbonyl branch where the end-product is a carbonyl group (Schuchmann & Müller, 2014). These two branches bind together when the enzyme complex carbon monoxide dehydrogenase/acetyl-CoA synthase drives the reaction where acetyl-CoA is formed (Schuchmann & Müller, 2014). Figure 1 illustrates the Wood-Ljungdahl pathway.

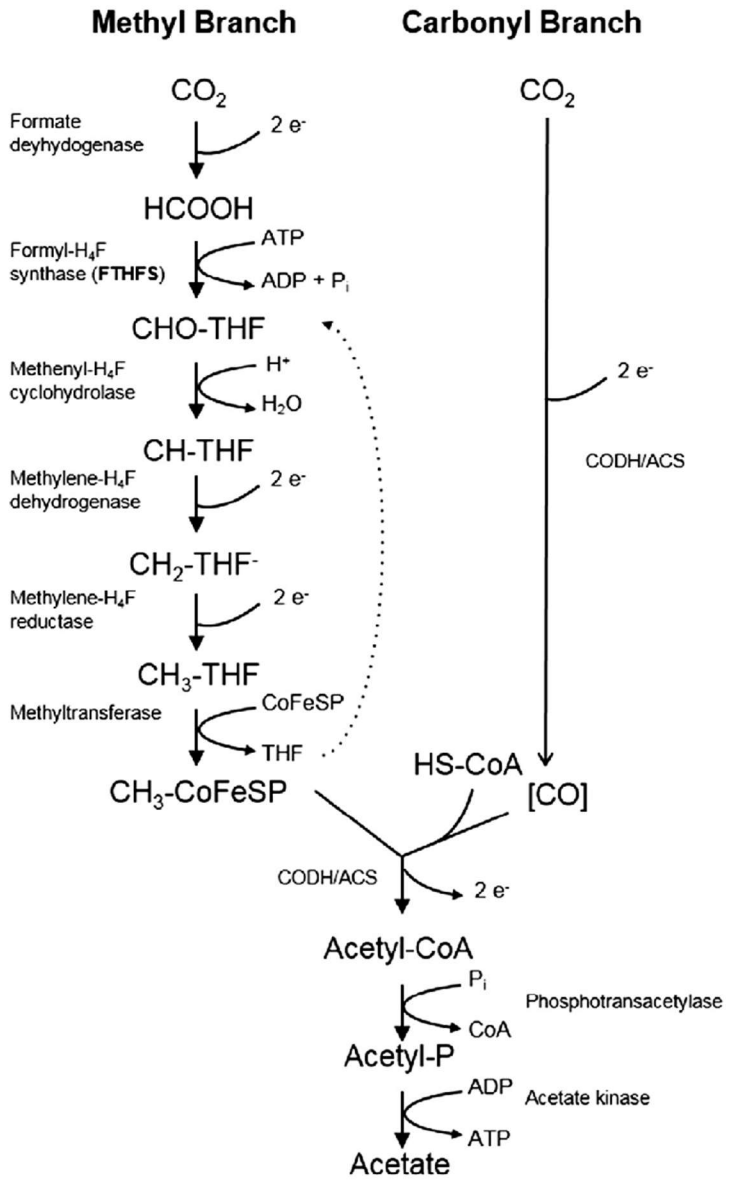

Figure 1. The Wood-Ljundahl pathway as described for C. ljungdahlii. HCOOH is formic acid, THF is tetrahydrofolate, CHO is formyl, CH is methenyl, CH_2 is methylene, CH_3 is methyl, CoFeSP is corrinoid iron-sulphur protein, CODH/ACS is carbon monoxide dehydrogenase/acetyl-CoA synthase, HS-CoA is Coenzyme A with its sulfhydryl group, ATP is adeninetriphosphate, ADP is adeninediphosphate, Pi is a phosphate group. As can be seen the THF is recycled once the CoFeSP molecule is bound to the methyl. CoA is also recycled when the acetyl group binds to the phosphate group. Adapted from (Westerholm et al., 2016).

1.2.2 Energy conservation mechanism of acetogens

The WLP is linked to the energy conservation inside the cell but it is not directly responsible because there is no net production of ATP throughout its reactions (Liew et al., 2016; Schuchmann & Müller, 2014). In *C. ljungdahlii*, and in many other microorganisms, it is instead another mechanism for energy conservation that has been found. It is through electron bifurcation and the directly responsible enzyme complexes called the Rnf complex and the ATPase that energy is conserved (Schuchmann & Müller, 2014). An overview of this energy conservation mechanism in *C. ljungdahlii* can be seen in figure 2.

1.2.2.1 The Rnf complex and the ATPase

Both the Rnf complex and the ATPase are membrane embedded protein complexes. The Rnf (ferredoxin:NAD^+ oxidoreductase) complex consists of several subunits and catalyses the oxidation of 1 reduced ferredoxin while 1 NAD^+ is reduced (Schuchmann & Müller, 2014). Using the energy of this reaction *C. ljungdahlii* can transfer 2 moles of H^+ out over the cell membrane and build up a chemiosmotic ion gradient (Schuchmann & Müller, 2014). The ATPase, an F_0F_1 ATP synthase, uses this ion gradient and generates ATP inside the cell by phosphorylating ADP (Schuchmann & Müller, 2014). For every ATP produced, 4 H^+ is transferred in through the ATPase (Schuchmann & Müller, 2014). This means that for every reduced ferredoxin that is oxidized by the Rnf, 0.5 ATP is produced. This also means that it is important to have a high Fd_{red}/NAD^+ ratio because the more reduced ferredoxin is available, the more ATP can be produced (Liu et al., 2020; Schuchmann & Müller, 2014).

1.2.2.2 The electron bifurcating hydrogenase HydABC and the electron bifurcating transhydrogenase Nfn

In *C.ljungdahlii*, production of reduced ferredoxin is done by the electron-bifurcating hydrogenase, HydABC (Schuchmann & Müller, 2014). HydABC is also important for *C.ljungdahlii* because it enables it to produce NADH. HydABC is a soluble and multi-subunit enzyme in which at least one unit binds a flavin cofactor. HydABC uses the mechanism flavin-based electron bifurcation which enables HydABC to oxidize H_2 and deliver the electrons to the connected and simultaneous reductions of ferredoxin and NAD^+ (Schuchmann & Müller, 2014). The reduction of NAD^+ is exergonic and thus enables the endergonic reduction of ferredoxin (Schuchmann & Müller, 2014). The finding of an electron bifurcating transhydrogenase, Nfn, has also been reported in *C. ljungdahlii*. Nfn oxidizes 1 reduced ferredoxin and 1 NADH to produce 2 NADPH (Schuchmann & Müller, 2014), and it is important for *C.ljungdahlii* because it directly connects the pools of ferredoxin and NADH to the pool of NADPH.

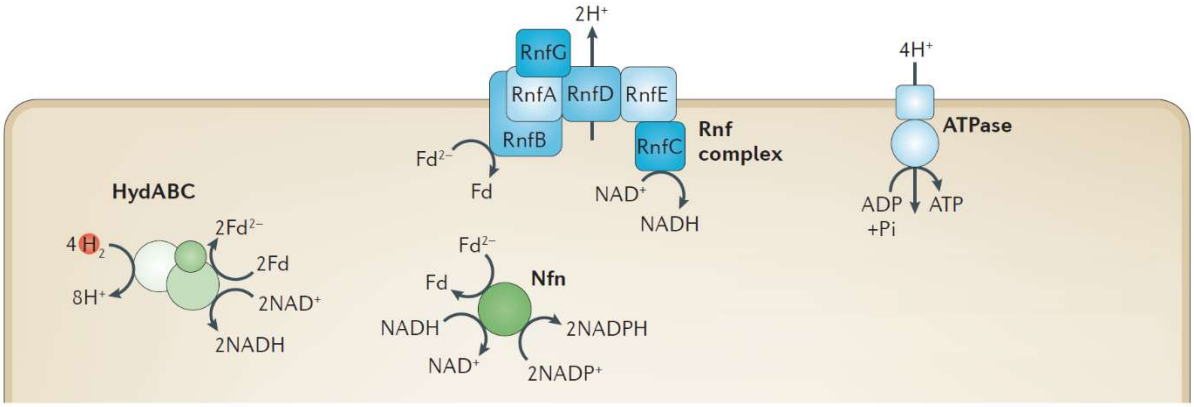

Figure 2. Illustration of the components that make up the energy conservation mechanism in C. ljungdahlii. HydABC is the hydrogenase allowing usage of hydrogen, the Rnf-complex with all its subunits allows the build-up of a proton gradient so that the ATPase can produce ATP. The Nfn-complex allows exchange between the different electron carriers. Fd is ferredoxin, NADPH is nicotinamide adenine dinucleotide phosphate, Pi is a phosphate group, NADH is nicotinamide adenine dinucleotide + hydrogen. Adapted from (10).

1.2.3 Ethanol production

An understanding of ethanol production in *C. ljungdahlii* is of importance in this report because it is a desired product from syngas fermentation since it can be used as a biofuel. Two pathways for ethanol production have been found which are illustrated in figure 3. These are the AOR (acetaldehyde:ferredoxin oxidoreductase) pathway and the AdhE (aldehyde/alcohol dehydrogenase) pathway (Liu et al., 2020). If ethanol is produced via the AOR pathway, acetate and acetaldehyde are first formed (Liu et al., 2020). The AOR enzyme is responsible for catalysing the production of acetaldehyde from acetate. This reaction is reversible using ferredoxin as an electron carrier (Liu et al., 2020). The AdhE pathway shares the same reaction from acetaldehyde to ethanol but there is only one reaction from acetyl-CoA to the acetaldehyde. Both reactions are reversible, catalysed by AdhE enzymes which both use NADH as electron donors (Liu et al., 2020).

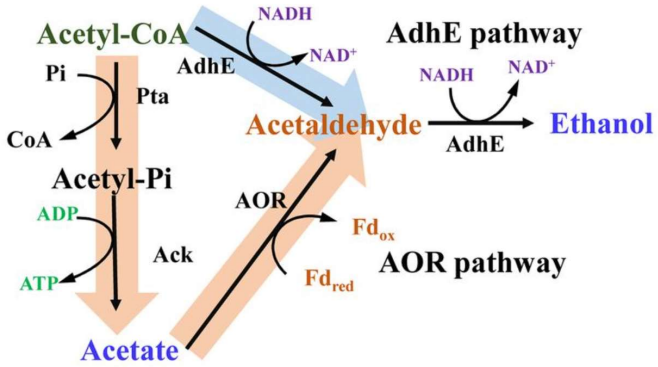

Figure 3. The AdhE and AOR pathways for ethanol production from acetyl-CoA in C. ljungdahlii. Reactions are reversible. AdhE is aldehyde/alcohol dehydrogenase, AOR is acetaldehyde:ferredoxin oxidoreductase, Fd is ferredoxin, NADPH is nicotinamide adenine dinucleotide phosphate, Pi is a phosphate group, NADH is nicotinamide adenine dinucleotide + hydrogen. Adapted from (11).

Ethanol production has been argued to depend on intracellular concentration of undissociated acetic acid, and how well *C. ljungdahlii* is growing (Richter et al., 2016). If *C. ljungdahlii* is growing and the intracellular concentration of undissociated acetic acid reaches a thermodynamic threshold, the acetic acid can be used to produce more biomass (Richter et al., 2016). During growth, there is also a need to balance the high amounts of NADH that is produced by the by the Rnf complex when the ATPase is producing ATP. Since ethanol production through the AdhE pathway requires 2 NADH, it has been suggested that it serves as a solution to balance the levels of NADH (Liu et al., 2020).

If *C. ljungdahlii* on the other hand is not able grow and there is an excess intracellular concentration of undissociated acetic acid, the acetic acid can be redirected to form ethanol (Richter et al., 2016). Reducing equivalents are then redirected toward ethanol production rather than biomass production. This shift can thus be induced by stressing the cell and by adding acetic acid to the medium, because undissociated acetic acid can diffuse over the cell membrane (Richter et al., 2016). It has also been suggested that when there are low amounts of reducing equivalents, the ethanol is oxidized back to produce more reducing equivalents (Liu et al., 2020). Because oxidizing ethanol to acetate through the AdhE

pathway gives 2 NADH and 1 ATP, and through the AOR pathway gives 1 NADH and 1 reduced ferredoxin (Liu et al., 2020).

1.2.2 Lactate and 2,3-butanediol production

2,3-Butanediol and lactate are two chemicals of interest in this report because they have been proven to be produced by *C. ljungdahlii* growing on syngas (Köpke et al., 2011). 2,3-Butanediol can be used as a precursor to produce methyl ethyl ketone and 1,3-butadiene, which can be used to produce nylon and synthetic rubber (Michael Köpke, Monica L. Gerth, Danielle J. Maddock, Alexander P. Mueller, FungMin Liew, Séan D. Simpson, 2014). Lactate can be used for production of biodegradable polylactic acid and polyester (Dai et al., 2017). The pathway for production of lactate and 2,3-butanediol in *C. ljungdahlii* can be seen in figure 4. As can be seen in figure 4, it is pyruvate that serves as precursor for both products (Hermann et al., 2021). Lactate is produced directly from pyruvate via the enzyme lactate dehydrogenase consuming the reducing equivalent NADH (Hermann et al., 2021). To produce 2,3-butanediol from pyruvate there are two intermediaries produced first. Acetolactate is produced first via the enzyme acetolactate synthase. Acetoin is then produced from acetolactate via the enzyme acetolactate decarboxylase. Lastly, 2,3-butanediol is produced from acetoin via the enzyme 2,3-butanediol dehydrogenase which consumes the reducing equivalent NADPH (Hermann et al., 2021). It is thought that the reason for lactate and 2,3-butanediol production in *C. ljungdahlii* is to decrease the levels of reducing equivalents and deacidification of pyruvic acid (Köpke et al., 2011).

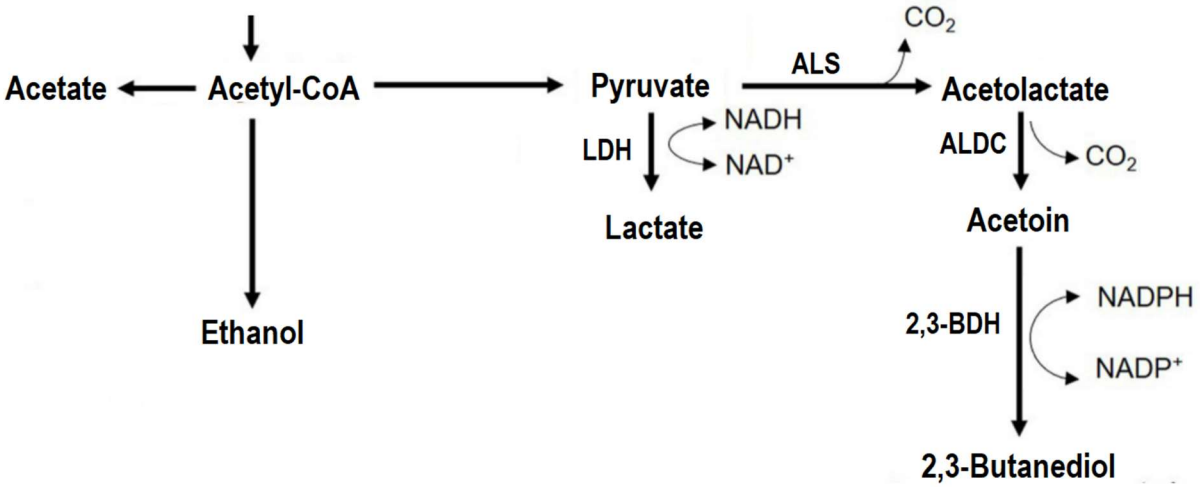

Figure 4. Pathway for lactate and 2,3-butanediol production from acetyl-CoA. Pyruvate is produced from acetyl-CoA, which enables the production of lactate, acetolactate, acetoin, and finally 2,3-butanediol. LDH is lactate dehydrogenase, ALS is acetolactate synthase, ALDC is acetolactate decarboxylase, 2,3-BDH is 2,3-butanediol dehydrogenase, NADPH is nicotinamide adenine dinucleotide phosphate, NADH is nicotinamide adenine dinucleotide + hydrogen. Adapted from (Hermann et al., 2021).

1.3 Bio-electrochemical systems

H_2 in syngas can provide for the reducing equivalents that are needed to reduce CO_2 and fix the carbon (Liew et al., 2016). But reducing equivalents can also be attained by directly using an electrode inside the fermentation broth (Barbosa et al., 2021; Liew et al., 2016). Using an electrode to provide more reducing equivalents can help both microbial growth and production of wanted chemicals (Barbosa et al., 2021). If the electric power supply is coming from renewable energy sources such as solar and wind power, the produced biofuels can serve as a storage of energy because low-carbon liquid fuels are energy dense and do not lose energy over time (Karthikeyan et al., 2019; Liew et al., 2016).

Combining bio-based catalysts, such as a microorganisms, with an electrochemical method to improve the reducing or oxidizing metabolism is what a bio-electrochemical system is (Zheng et al., 2020). The microorganism should be capable of accepting or donating electrons from or to solid inorganic compounds, such as an electrode (Karthikeyan et al., 2019). A bio-electrochemical system can be composed by two chambers separated by a membrane (Barbosa et al., 2021). One chamber contains the anode, and the other contains the cathode. One of these electrodes is set to be the working electrode, and the other is the counter electrode. A reference electrode is also used because a reference is needed to measure the potential of the working electrode (Elgrishi et al., 2018). The cathode and the anode are connected through an external circuit with a potentiostat controlling the potential of the electrodes. It is possible to have microorganisms in either chamber depending on the desired use (Barbosa et al., 2021). Figure 5 shows an illustration of a bio-electrochemical system.

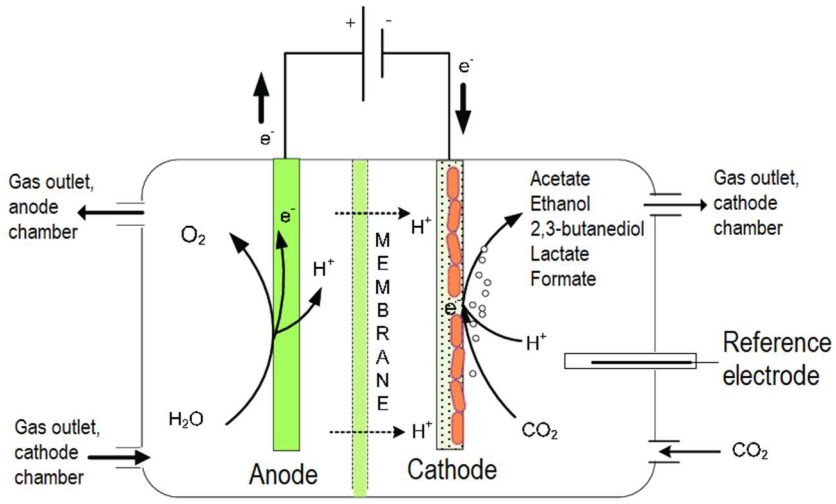

Figure 5. Illustration of a bio-electrochemical system in the form of microbial electrosynthesis. The anode and the cathode are connected through a potentiostat, and in this case microorganisms have attached to the cathode. A reference electrode is inserted next to the cathode. Protons diffuse through the membrane from the anode chamber to the cathode chamber. In this case, CO_2 gas is inserted into the cathode chamber, and the outlet gas from the cathode chamber is the inlet gas to the anode chamber. Adopted from (Bajracharya, 2016).

1.3.1 Applications of bio-electrochemical systems

A bio-electrochemical system mainly involves three different applications. These are microbial electrolysis cells, microbial fuel cells, and microbial electrosynthesis cells (Karthikeyan et al., 2019). A microbial fuel cell is a type of a bio-electrochemical system where electricity is produced. This is done by having a biocatalyst, an electroactive microorganism, in the anode chamber so that it can oxidize a compound and transfer the electrons to the anode (Barbosa et al., 2021; Karthikeyan et al., 2019). From the anode, the electrons flow through an external circuit to the cathode so that electricity is produced (Barbosa et al., 2021). Protons also flow from the anode chamber to the cathode chamber but through the membrane to balance the charge. In a microbial electrolysis cell, energy is instead required to set a potential at the cathode so that the protons are reduced to hydrogen gas (Badwal et al., 2014; Karthikeyan et al., 2019). In microbial electrosynthesis a potential is also set at the cathode but for the reduction of CO_2 so that multi-carbon compounds can be produced by microorganisms (Nevin et al., 2011). *C. ljundahlii* is an example of an organism that has been inoculated into the cathode chamber and used for microbial electrosynthesis (Nevin et al., 2011).

It is also possible to affect different metabolic pathways in electroactive microorganisms to alter the production of metabolites of the organism. This is done by introducing a potential on the microorganism so that intracellular redox balances are affected which then affect metabolic pathways of the organism (Barbosa et al., 2021). This process is called electro fermentation and can give a higher yield of a wanted product compared to not using an electrode. 1,3-propanediol production was increased by 25 percent in one study by using an electrode compared to not using an electrode (Barbosa et al., 2021). Product formation from one type of product can also be shifted to another product. *C. autoethanogenum* that is a specie closely related to *C. ljungdahlii* had a shift in produced products in an electro fermentation (Barbosa et al., 2021). Less acetate, but more lactate and 2,3-butanediol were produced.

1.3.2 Electron transfer

The exact electron transfer mechanism between the electrode and the microorganism is not known but it can be direct or mediated (Barbosa et al., 2021; Jiang et al., 2019; Karthikeyan et al., 2019). Figure 6 illustrates the different possible mechanisms. The working potential of the electrode largely influences the transfer mechanism (Jiang et al., 2019), but microorganisms that cannot connect to the electrode use mediated electron transfer (Barbosa et al., 2021). Mediated electron transfer means using redox active molecules as mediators. They function as electron shuttles across the cell membrane and can be self-secreted, in-situ generated or added to the medium (Barbosa et al., 2021; Jiang et al., 2019).

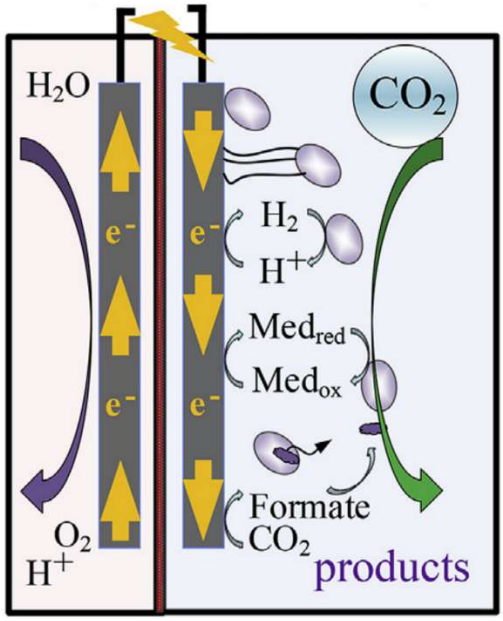

Figure 6. The different possible electron transfer mechanisms of electron receiving microorganisms at the cathode. Direct transfer to the microorganism that have formed a monolayer biofilm or connected through pili's, and indirect using H_2, formate or another mediator. The left side is the anode chamber with and anode inside, and the right side is the cathode chamber with a cathode inside. Adapted from (14)

In-situ generated H_2 and formate are two examples of electron mediators (Karthikeyan et al., 2019). H_2 has low solubility but when it has been generated, acetate production has been improved of (Karthikeyan et al., 2019). Formate is to the contrary is very soluble but is generated at lower potentials than H_2 so its production uses more electrical energy than H_2 (Karthikeyan et al., 2019). Formate can go directly into the Wood-Ljungdahl pathway but also be converted to CO_2 to produce reducing equivalents in the cell. There are electron shuttles which require less electrical energy, such as ammonia and Fe^{2+} but they have lower electron transfer rates (Karthikeyan et al., 2019). Other options include neutral red, methyl viologen, and thionin (Karthikeyan et al., 2019).

Microorganisms that can physically connect to the electrode can instead transfer electrons directly to and from the electrode (Barbosa et al., 2021; Karthikeyan et al., 2019). If the microorganism is forming c-type outer membrane cytochromes, and a monolayer biofilm on the electrode; the electron transfer can happen via the cytochromes (Barbosa et al., 2021). If the microorganism is forming a multilayer biofilm, the transfer can happen via conductive pili formed on some of the microorganisms (Barbosa et al., 2021). The pili enables long range electron transfer which is useful since some microorganisms will naturally be further away from the electrode in a multilayer biofilm (Karthikeyan et al., 2019). An example of a microorganism that has been shown to be capable of direct electron transfer is *C. ljungdahlii*, which produced acetate at a potential of -400 mV (Karthikeyan et al., 2019). There is however a need for further investigation to better understand the electron transfer between acetogens and electrodes.

1.3.3 Bio-electrochemical analysis techniques

Two bio-electrochemical analysis techniques are of importance for this report. These are cyclic voltammetry and chronoamperometry.

1.3.3.1 Cyclic voltammetry

Cyclic voltammetry is used to study chemical species in a solution. For a cyclic voltammetry a three-electrode set-up as described for the bio-electrochemical system is used. That is with a working electrode, a counter electrode, and a reference electrode (Harnisch & Freguia, 2012). Cyclic voltammetry is based on the principle that there are two different types of current that can flow. Capacitive currents and faradaic currents. A capacitive current is a balancing current that occurs when the charge density at the electrode/electrolyte interface is changed when the potential is changed (Elgrishi et al., 2018). A capacitive current is also known as a background current. Faradaic currents instead occur when there is an oxidation or reduction reaction (Elgrishi et al., 2018).

A cyclic voltammetry is operated by applying a potential that is linearly dependent on time on the working electrode (Elgrishi et al., 2018). A starting potential is set as well as a final potential and a scan rate. The potential then changes from the starting value to the final value and back to the starting value with the scan rate. The generated current is a function of the potential, and it is measured. Plotting the current as a function of the potential gives a cyclic voltammetry curve (Elgrishi et al., 2018). See figure 7 for illustration.

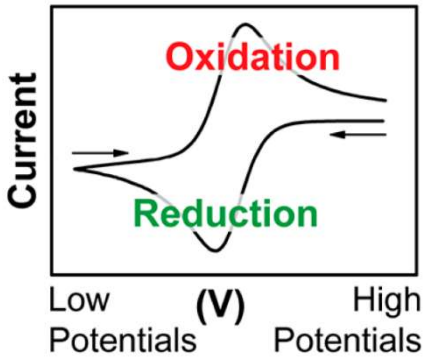

Figure 7. A cyclic voltammetry curve where the current is a function of the potential. The potential (V) is going from the starting potential to the final potential before returning to the starting potential. Current peaks are observed when a chemical species is oxidated when the potential is going from lower to higher potential, and when the chemical species is reduced when the potential is going from a higher potential to a lower. Adapted from (Elgrishi et al., 2018).

In a cyclic voltammetry curve, when starting from the initial potential there is no sudden change in the level of current because there is only capacitive background current. The sudden change in current level comes when an oxidation or reduction occurs at a specific potential (Elgrishi et al., 2018). If the potential has been moving from a more negative potential to a more positive potential, the current level will increase until it has reached a maximum and then decrease when there are less of the chemical species remaining to be oxidized (Elgrishi et al., 2018; Harnisch & Freguia, 2012). Then the potential reaches the final potential and reverses back to the starting potential. On the way back to the starting potential, the current will decrease and reach a minimum at approximately the same potential as where there was an increase. It will then again increase to the level before the decrease when there are less of the chemical species remaining to be reduced. The

potentials at the maximum and minimum current levels are called the anodic peak potential (E_{pA}) and the cathodic peak potential (E_{pC}), respectively (Elgrishi et al., 2018).

1.3.3.2 Chronoamperometry

Chronoamperometry is an analysis technique where current is recorded as a function of time (Allen J. Bard, 2001). It is used for extracting quantitative information (Patil et al., 2014). In the type of chronoamperometry used for this report, a set potential is used, and the current levels are recorded. This means that the current consumption can be monitored in the cathodic chamber if the cathode is used as the working electrode, at a determined potential.

1.4 Aim

Clostridium ljungdahlii is a microorganism that has proven to be able to produce ethanol in syngas fermentation. It has also been proven to be able to consume current during microbial electrosynthesis to produce acetate. It is also known that different cathodic potentials can affect the bio-electrochemical activity of electroactive microorganisms differently. Thus, it is of interest to investigate the bio-electrochemical activity of *Clostridium ljungdahlii* at different cathodic potentials, and this will be done in this report.

The objectives are thus:

- To perform microbial electrosynthesis in a bio-electrochemical system with *Clostridium ljungahlii* at the potentials -400 mV, -600 mV, -800 mV and -1000 mV.
- To perform an abiotic bio-electrochemical system experiment at the potentials -400 mV, -600 mV, -800 mV and -1000 mV to compare with the microbial electrosynthesis.
- To perform serum flask control experiments to obtain better understanding of the results from the bio-electrochemical system experiments.
- To analyse the results in terms of product formation, growth, pH, current consumption, and redox species present in the bio-electrochemical system reactors.

2. Materials and methods

The materials and methods used for the experiments to investigate the bio-electrochemical activity of *Clostridium ljungahlii* are described in this chapter. Figure 8 gives an overview of the process of the investigation, which shows that three types of experiments were conducted: biotic bio-electrochemical experiments, abiotic bio-electrochemical experiments, and serum flask control experiments.

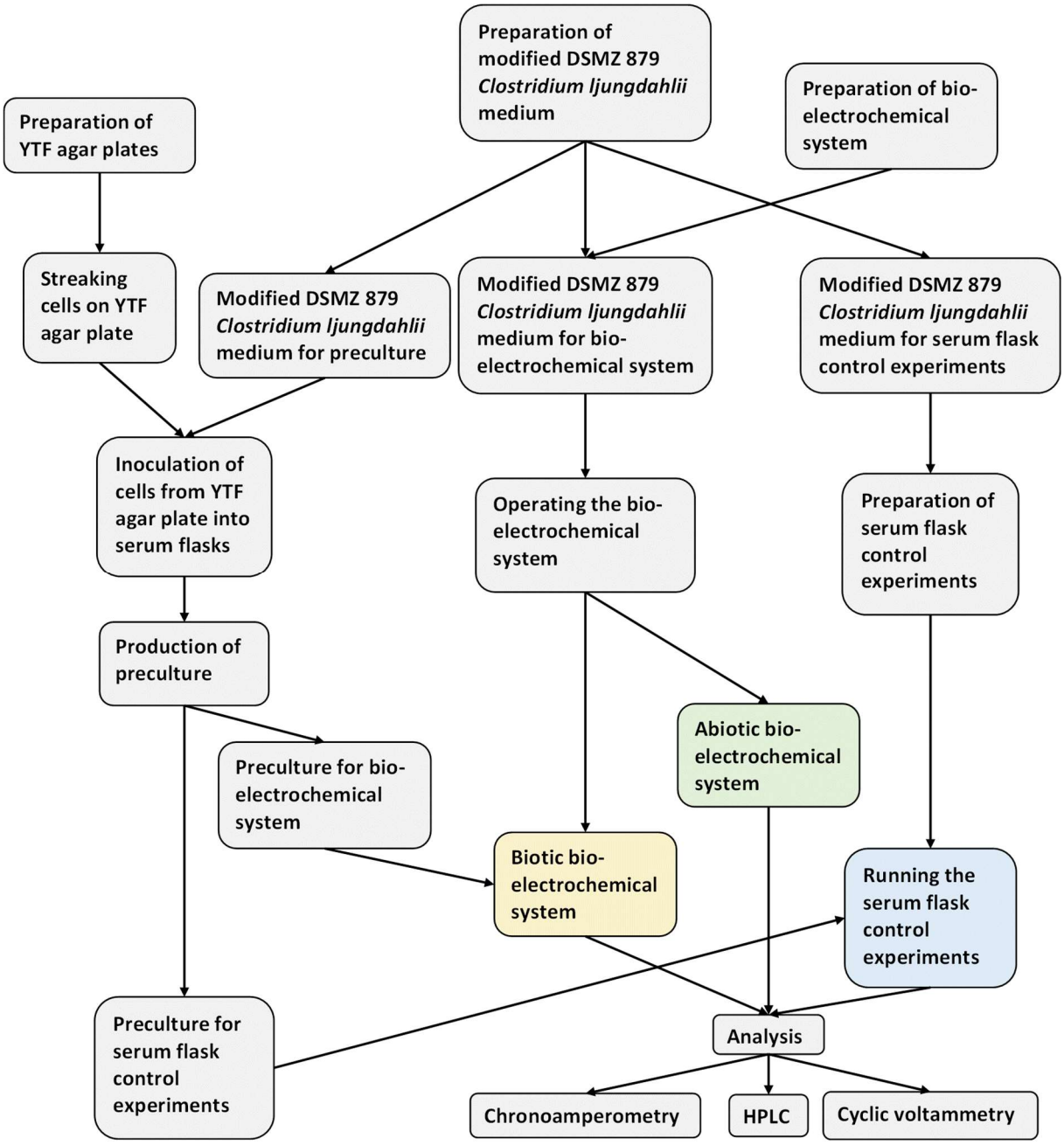

Figure 8. Overview of the methods used in this report to investigate the bioelectrochemical activity of C. ljungdahlii. The three types of experiments were biotic bioelectrochemical system experiments, abiotic bioelectrochemcal system experiments and serum flask control experiments, and were performed in the respective order. These experiments are marked with their respective colours in the figure, yellow, green, and blue. The other steps listed are preparation steps for preparing the three experiments. YTF is short for Yeast Tryptone Fructose, HPLC is short for high-performance liquid chromatography, and DSMZ is short for Deutsche Sammlung von Mikroorganismen und Zellkulturen.

2.1 Biotic bio-electrochemical system

In this section the procedure for performing the biotic bio-electrochemical system is described from the preparations for the experiment until the analysis of the results.

2.1.1 Preparation of YTF agar plates

Agar medium with components according to table 1 were prepared and autoclaved before it was stored in 62 °C for two days and then later poured in agar forms in a sterile LAF bench. The agar plates were then stored in the fridge.

Table 1. Listed components for YTF agar plates for 1 L medium.

Yeast extract	10 g
Bacto Tryptone	16 g
Fructose	10 g
NaCl	0.20 g
Vitamin solution	1 mL
Agar	15 g
Distilled water	1000 mL

2.1.2 Streaking cells on YTF agar plates

One agar plate was then put inside an anaerobic chamber with 37 °C, containing 10:10:80 H_2:CO_2:N_2 gas, over-night. Frozen glycerol stock of *Clostridium ljungdahlii* was streaked on the agar plate inside anaerobic chamber next day. The plate was stored until distinct colonies could be seen.

2.1.3 Preparation of modified DSMZ 879 Clostridium ljungdahlii medium

Medium was prepared according to the DSMZ 879 *Clostridium ljungdahlii* medium with modifications. The content and their respective amounts for this medium can be seen in table 2. NH_4Cl, KCl, $MgSO_4 \times 7H_2O$, NaCl and $CaCl_2 \times 2H_2O$ had already been prepared in a 1000X solution.

Table 2. Listed components for making the modified DSMZ 879 medium.

NH_4Cl	1 g
KCl	0.1 g
$MgSO_4 \times 7H_2O$	0.2 g
NaCl	0.8 g
$CaCl_2 \times 2H_2O$	0.02 g
Trace element solution (*Appendix A1)	10 mL
Na-resazurin solution (0.1% w/v)	1 mL
Vitamin solution 1000X (*Appendix A2)	1 mL
MES monohydrate buffer	20 g
$FeSO_4 \times 7H_2O$	50 mg
Sodium acetate	0.25 g
L-Cysteine-HCl x H_2O	0.6 g
Distilled water	1000 mL

2.1.4 Preparation of modified DSMZ 879 Clostridium ljungdahlii medium for preculture

For the preculture, the pH of the medium was set to 5.7 with NaOH when the components listed in table 2 had been mixed. 40 mL of the medium was then inserted into a 200 mL serum flask before closing it with a butyl rubber stopper and sealing with an aluminium crimp seal. To remove oxygen from the headspace before sterilization with autoclave, the air was changed for 100 percent N_2 gas with a gas exchanger (G.R. Instruments). The gas in the headspace volume of the flask was then again changed with 100 % N_2 while the medium was hot after sterilization. After the medium had cooled down in the fridge the serum flask was injected with 1 percent volume per volume of a solution of 10 g KH_2PO_4 per 1000 mL distilled water. It was also injected with a gas mixture of 2 bar 80:20 H_2:CO_2 gas, and stored over-night in a still and dark incubator with 37 °C.

2.1.5 Inoculation of cells from YTF agar plate into serum flasks

The serum flask was then brought into the anaerobic chamber, having a gas mixture of 10:10:80 H_2:CO_2:N_2, so that *C. ljungdahlii* could be inoculated into the flask. The inoculation process was performed accordingly. 800 µl PBS buffer was first inserted into a sterile 1.5 mL falcon tube before picking a colony off the agar plate and inserting it into the PBS, with a pipette. The PBS solution was mixed by pipetting up and down before it was inoculated into the serum flask containing the modified DSMZ 879 medium. The inoculation was done with a 1 mL syringe and needle to maintain the headspace pressure. The serum flask was then taken out from the anaerobic chamber and put on its side into a rotating incubator at 160 rpm and 37 °C. Figure 9 shows the type of 200-mL serum flask used in this work.

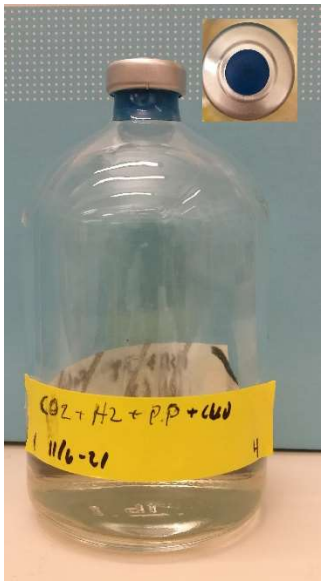

Figure 9. 200-mL serum flask filled with 40 mL modified DSMZ 879 medium, 1 percent KH_2PO_4 and inoculated with C. ljungdahlii. Headspace is filled with 80:20 H_2:CO_2 gas, and the flask is closed with a rubber stopper and sealed with an aluminium crimp seal.

2.1.6 Production of preculture

For production of pre-culture, the cells grown in the 200-mL serum flasks that was inoculated from the agar plates were inoculated into 1-L and 500-mL serum flasks. Both the 1-L and 500-mL flasks contained the same medium as the 200-mL flasks and were treated in the same manner as the 200-mL flasks. The difference was that their volumes were set to

240 and 120 mL, respectively. One 1-L serum flask and two 500-mL serum flasks were used, and they were inoculated on the day after they were prepared.

The 1-L serum flask was inoculated with an OD of 0.008 and it was done in the anaerobic chamber with a 10-mL syringe and needle. The syringe was rinsed twice with the cell broth from the 200-mL serum flask to minimize oxygen contamination from the needle and the syringe. The same process was performed on the next day for the first 500-mL serum flask but with an initial OD of 0.01. The second 500-mL serum flask was also inoculated with an OD of 0.01 but it was done in a LAF bench. Syringe and needle were used again, but they were rinsed twice with a $H_{18}Na_2O_9S$ solution to remove excess oxygen. The 1-L serum flask and the first 500-mL serum flask were then again filled with 80:20 H_2:CO_2 gas before put on their side inside a shaking incubator at 37 °C and 135 rpm. The second 500-mL serum flask was also put inside a shaking incubator at 37 °C, but at 139 rpm and it was not again filled with gas after inoculation.

Growth was observed after 10 days in the 1-L serum flask and the second 500-mL flask and they were once again filled with 80:20 H_2:CO_2 gas. The first 500-mL flasks showed growth after 4 weeks so it was too filled with 80:20 H_2:CO_2 gas then. It was also injected with 140 mL extra equally treated medium to increase the volume of preculture.

2.1.7 Preparation of bio-electrochemical system

The BES was prepared by first connecting two Duran borosilicate glass bottles with a Nafion proton exchange membrane in between. The ports of the flasks were then closed with closed caps except for the upper left and lower right ports, see figure 10, which were closed with caps with rubber stoppers. The upper left was used for sampling and inoculation while the lower right was used to flush the bottle with CO_2 gas. The top openings of both chambers were closed with butyl rubber stoppers. The butyl rubber stopper of the left chamber was punctured with titanium wire from which a carbon block (11x21.5x51 mm) was hanging. The carbon block was used as the cathode. The butyl rubber stopper of the right chamber was on the other hand punctured with a platinised titanium rod functioning as the anode. Finally, the top butyl rubber stopper of the cathode chamber was punctured with a large needle for sparging the cathode chamber with the CO_2 gas. The large needle was also connected to a tube and filter. Tubes for connecting the cathode chamber with the anode chamber, as can be seen in figure 10, were also prepared.

Ag/AgCl reference electrodes were then controlled to see if they had a smaller difference in potential than 20 mV compared to another Ag/AgCl reference electrode set as the reference.

Subsequently, medium was prepared for the anode and cathode chamber. The medium was the same as previous modified DSMZ 879 *C. ljungdahlii* medium but with two modifications. The Na-resazurin solution was not added and the pH was lower. A pH of 5.0 for the cathode chamber and a pH of approximately 3.2 in the anode chamber. Respective medium was filled into respective chamber. 250 mL in the anode chamber and 210 and 215 mL in the cathode chamber for the first and second batch of reactors, respectively. The tube connected to the large needle was closed with a screw clamp and the open end of the filter was plugged with

cotton wool before it was wrapped in aluminium foil. Lastly, the reactors, the tubes for connecting the anode chamber with the cathode chamber, and caps for inserting the reference electrodes were autoclaved.

After the sterilization with the autoclave, the reference electrodes were inserted into the cathode chamber in a LAF bench. The electrodes were sterilized by first by placing them in 70 percent ethanol for 10 minutes and the dipping them in 100 percent ethanol before passing them over a flame.

While the reactors were still warm, they were connected to the CO_2 gas through the attached tube on the cathode chamber. This was done inside an incubator with 37 °C. A needle was also inserted into the top butyl rubber stopper to avoid too high pressures. This needle was then used to connect to the anode chamber through the tubes earlier described. When both chambers were being sparged with CO_2 gas, they were injected with 1 percent volume per volume KH_2PO_4 solution. The potentiostat was then connected to the reactor and chronoamperometry programs with respective potentials were started to polarize the reactors over-night.

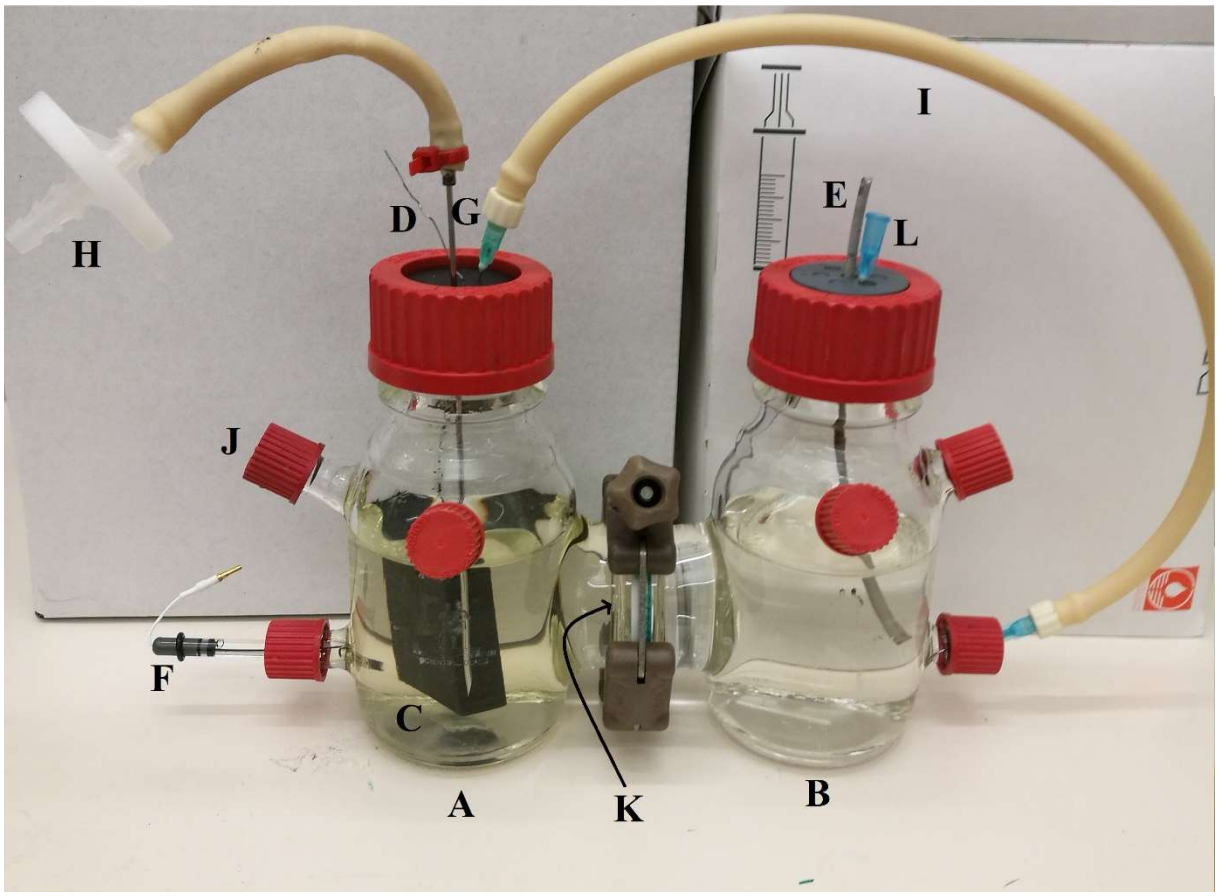

Figure 10. Set-up of the bio-electrochemical system before connecting to CO2 gas and potentiostat. A: Cathode chamber; B: Anode chamber; C: Carbon block used as cathode; D: Titanium wire connected to the cathode; E: Platinised titanium rod used as anode; F: Ag/AgCl reference electrode; G: Needle used for sparging CO_2; H: Filter for inlet CO_2 gas; I: Tube leading gas from cathode chamber to anode chamber; J: Sampling port; K: Nafion proton exchange membrane between cathode and anode chamber.

2.1.8 Operating the bio-electrochemical system

When the reactors were polarized the cells were inoculated from the preculture serum flasks. A 60 mL sterile syringe was rinsed twice with a $H_{18}Na_2O_9S$ solution to remove excess oxygen before it was used for inoculation of the cells. For the first BES experiments with four reactors set at -400 mV, -400 mV, -400 mV and -600 mV; 40 mL *C. ljungdahlii* culture with an OD of 0.243 was inoculated from the 1-L serum flask described in section *Production of preculture*. For the second experiment with seven reactors, two reactors at -600 mV, three reactors at -800 mV and two at -1000 mV; 35 mL was inoculated with an OD of 0.523 from the first 500-mL serum flask that showed growth. For the third experiment, three reactors at -1000 mV were inoculated with 35 mL with an OD of 0.684 from the second 500-mL flask that showed growth. The chronoamperometry was then started and measurements of the potentials between the reference electrodes and the cathodes and the potentials between the cathodes and the anodes were performed. 1 mL samples were also taken from the sampling port in the cathodic chamber to measure the OD at 660 nm, pH, and store for HPLC. Sampling was performed every 24 hours for 14 days. After the final sampling time, the chronoamperometry was stopped and a cyclic voltammetry was started.

2.2 Abiotic bio-electrochemical system

The abiotic bio-electrochemical system experiments were performed in the same manner as the biotic bio-electrochemical system experiments, with four differences. Firstly, no cells were needed so no preculture were produced and no cells were inoculated. The volumes set for the for both the anode and cathode chambers were 250 mL from the start, OD was not measured and only a duplicate of reactors was operated for -1000 mV.

2.3 Serum flask control experiments

2.3.1 Preculture for serum flask experiments

The serum flask control experiments were performed biotically in contrast to the abiotic bio-electrochemical system experiments. The preculture was produced in the same manner as for the biotic bio-electrochemical system experiments but with one 1-L serum flask and one 200-mL serum flask. The 1-L flask contained 240 mL medium while the 200-mL flask contained 40 mL medium. Both flasks were inoculated with an OD of 0.01 in in a LAF bench with a syringe and needle that were rinsed twice with a $H_{18}Na_2O_9S$ solution. The flasks were not again filled with 80:20 H_2:CO_2 gas directly after inoculation when it was put on its side inside a shaking incubator at 37 °C and 141 rpm. Although they were filled with 80:20 H_2:CO_2 gas again after two weeks when growth could be observed.

2.3.2 Preparation of modified DSMZ 879 Clostridium ljungdahlii medium for serum flask control experiments

Different media were prepared for the serum flask control experiments listed in table 3. The medium for the first control experiment was prepared in the same manner as the medium for the preculture. The medium for the second serum flask control experiment was also prepared in the same manner, except that 1 bar 99.99 percent CO_2 gas was used. The medium for the third serum flask control experiment differentiated from the first by setting the pH to 5 instead of 5.7. The medium for the fourth serum flask control experiment also

differed from the first by having a pH of 5 instead of 5.7, but 50 mM formic acid was also injected.

Table 3. Conditions used for the serum flask control experiments compared to the production of preculture.

Conditions for serum flask control experiment
1. pH 5.7 and a gas mixture of 2 bar 80:20 H_2:CO_2.
2. pH 5.7 and 1 bar 99.99 percent CO_2 gas.
3. pH 5.0 and a gas mixture of 2 bar 80:20 H_2:CO_2.
4. pH 5.0, a gas mixture of 2 bar 80:20 H_2:CO_2 and 50 mM formic acid.

2.3.3 Running the serum flask control experiments

All the serum flask control experiments were performed in triplicates in 200-mL flasks with 40 mL medium. All three flasks of the first condition and two flasks of the second condition, were inoculated with an initial OD of 0.02 from the 1-L flask that had an OD of 0.273. The rest of the serum flasks were inoculated with an initial OD of 0.03 from the 40-mL preculture serum flask that itself had an OD of 0.430. One flask with the third condition accidentally lost some of its initial gas pressure upon inoculation. The experiment was operated for two weeks, and all the flasks were kept on their sides in a rotating incubator with 160 rpm and 37 °C. 1 mL samples were taken every 24 hours using syringe and needle to measure pH and save for HPLC.

2.4 Analysis

2.4.1 Chronoamperometry

The chronoamperometry was operated so that the current flow was recorded once every 60 seconds and plotted against time so that the current consumption could be followed. The data from the chronoamperometry was used so that the total current consumption was calculated by integrating the current graph. This was used to calculate the total charge provided from the potentiostat, which then was used to calculate the coulombic efficiency for each product produced.

The coulombic efficiency is a good performance index for production of desired chemicals in a bio-electrochemical system (Barbosa et al., 2021). Coulombic efficiency is the fraction of consumed electrons recovered into products. A low coulombic efficiency could be due to production of unwanted chemicals or production of cathodically evolved H_2. Microbial growth and maintenance also need electrons.

The coulombic efficiency was calculated according to equation 1 (Im et al., 2016).

$$CE(\%) = \frac{nFm}{\int_0^1 Idt} * 100\% \quad (1)$$

n is the theoretical amount of moles electrons needed per mole product. *F* is Faraday's constant which equals 96 485,3383 C/mol, and *m* is the amount of product produced in moles. *I* is the consumed current.

To know the amount of moles electrons needed per mole product, the electron balances for respective product shown through equations 2-6 were used. Equation 2 which displays the electron balance for acetate shows that 8 moles of electrons are needed to form 1 mole of acetate. Equations 3-6 displays the electron balances of ethanol, formic acid, 2,3-butanediol and lactate, respectively.

$$2CO_2 + 8H^+ + 8e^- \rightarrow CH_3COOH + 2H_2O \quad (2)$$

$$2CO_2 + 12H^+ + 12e^- \rightarrow C_2H_5OH + 3H_2O \quad (3)$$

$$CO_2 + 2H^+ + 2e^- \rightarrow HCOOH \quad (4)$$

$$4CO_2 + 20H^+ + 20e^- \rightarrow C_4H_{10}O_2 + 5H_2O \quad (5)$$

$$3CO_2 + 8H^+ + 8e^- \rightarrow C_3H_6O_3 + 3H_2O \quad (6)$$

2.4.2 Cyclic voltammetry

The cyclic voltammetry was operated in the range of -1.4 V and 0 V with a starting value of -0.6 V. The scan rate was set to 1 mV/s, and 5 cycles were performed.

2.4.3 HPLC

For analysing the product formation in each experiment, a JASCO UV RI HPLC system was used with a Rezex ROA-Organic Acid H + (8 %) LC column (300 x 7.8 mm). It was used with a UV detector with the oven temperature at 80 °C. The eluent was 5 mM H_2SO_4 with a flow rate of 0.8 mL/min.

3. Results

The results from the conducted experiments investigating the bio-electrochemical activity of *Clostridium ljungahlii* are presented in this chapter. The results from the biotic bio-electrochemical system experiment are presented in section 3.1 followed by the results from the abiotic bio-electrochemical system experiment in section 3.2, and the results from the serum flask control experiments in section 3.3.

3.1 Biotic bio-electrochemical system

The product formation, coulombic efficiency and the pH can be found in this chapter. Growth measurement data can be found in appendix A3 and supplied charge data in appendix A4.

3.1.1 Product formation

The products that were detected in the -400 mV reactors are acetate, formate, 2,3-butanediol and lactate. Figure 11 shows how the average concentration of these products vary with time. The concentration of acetate is shown on the primary y-axis while the concentrations of formate, 2,3-butanediol and lactate are shown on the secondary y-axis. The acetate concentration decreased by approximately 2 mM from 8.5 mM to 6.6 mM. The concentrations of the other products were all below 0.15 mM. The concentration of formate decreased from 0.14 mM to 0.05 mM, lactate concentration was kept constant at 0.04 mM, and 2,3-butanediol increased from 0 mM to 0.07 mM before decreasing to 0 mM again. The average 2,3-butanediol concentration showed a high variability with large error bars.

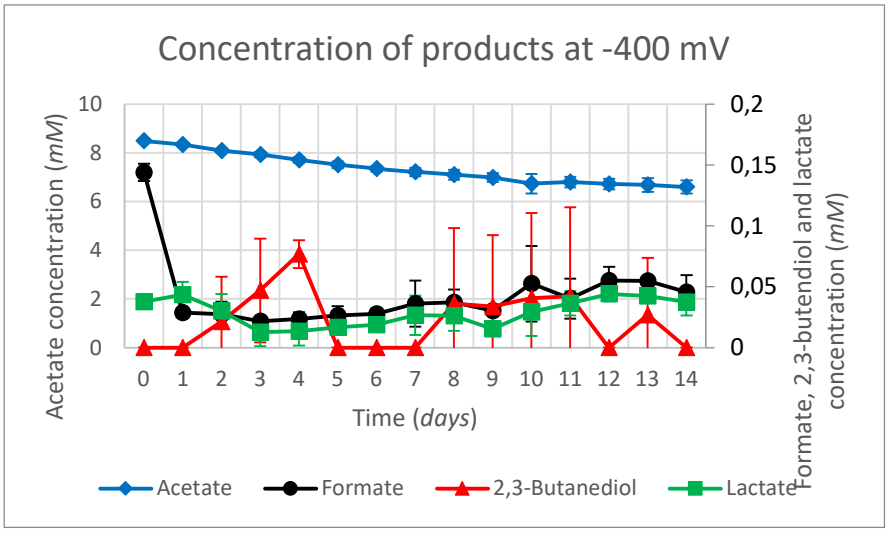

Figure 11. The average concentrations of the detected products acetate, formate, 2,3-butanediol and lactate at -400 mV during a time span of 14 days. The concentration of acetate can be read on the primary y-axis, while the concentrations of formate, 2,3-butanediol and lactate can be read on the secondary y-axis.

In the reactors with -600 mV the products acetate, ethanol, formate, 2,3-butanediol and lactate were detected. Figure 12 shows how the relationship between the average concentrations of the reproducible products acetate, formate and 2,3-butanediol varies with time. The concentration of acetate is shown on the primary y-axis while the concentrations of formate and 2,3-butanediol are shown on the secondary y-axis. As can be seen in figure 12, the acetate concentration increased from 8.31 mM to 9.55 mM. The concentration of

formate also increased, but from 0.24 mM to 0.60 mM. The 2,3-butanediol concentration on the other hand decreased from 0.02 mM to 0 mM even though higher concentrations were detected in between. However, with high error bars. The formate concentration profile also had high error bars.

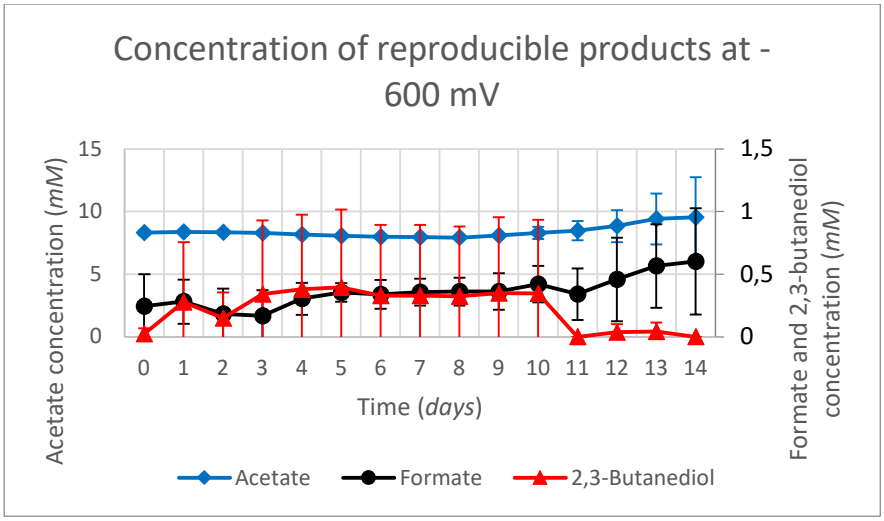

Figure 12. The concentration profiles at the potential -600 mV for the detected chemicals acetate, ethanol, formate, 2,3-butanediol and lactate during a time span of 14 days. The concentration of acetate can be read on the primary y-axis, while the concentrations of formate and 2,3-butanediol can be read on the secondary y-axis.

The concentrations of ethanol and lactate which could not be reproduced can instead be seen in figure 13. The lactate concentration changed from 0.06 mM to 0.14 mM while the ethanol concentration increased from 0 mM to 17.8 mM. While the lactate concentration is shown to be very low, the ethanol concentration is the highest of all the products at -600 mV.

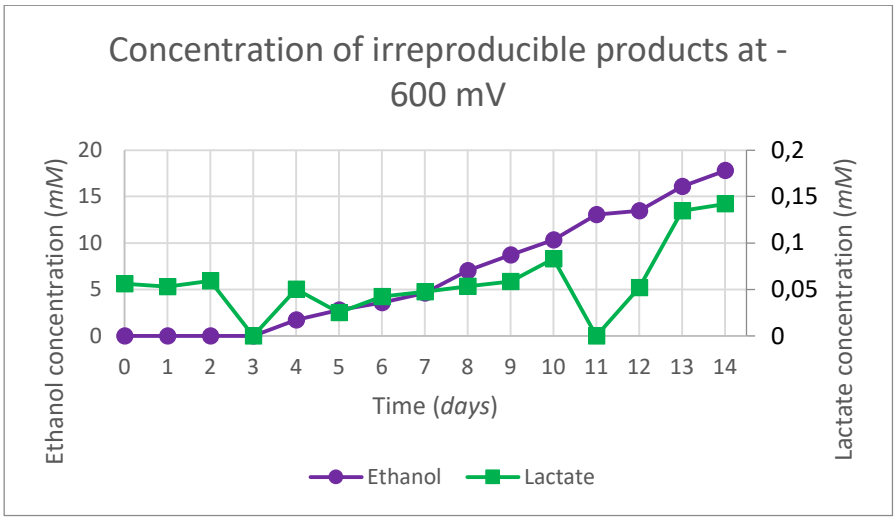

Figure 13. The concentrations of the detected but unreproducible products formate, acetate and 2,3-butanediol at -600 mV during a time span of 14 days. The concentration of ethanol can be read on the primary y-axis, while the concentrations of lactate can be read on the secondary y-axis.

In the reactors at -800 mV, only the products formate, acetate and 2,3-butanediol were detected. This can be seen in figure 14. There can be seen that the average concentrations of all the detected products increased. Formate increased from 1.25 mM to 24.53 mM, acetate

increased from 8.05 mM to 9.57 mM and 2,3-butanediol increased from 1.01 mM to 3.22 mM. While formate showed the highest concentrations, it also showed highest variability in concentration between reactors.

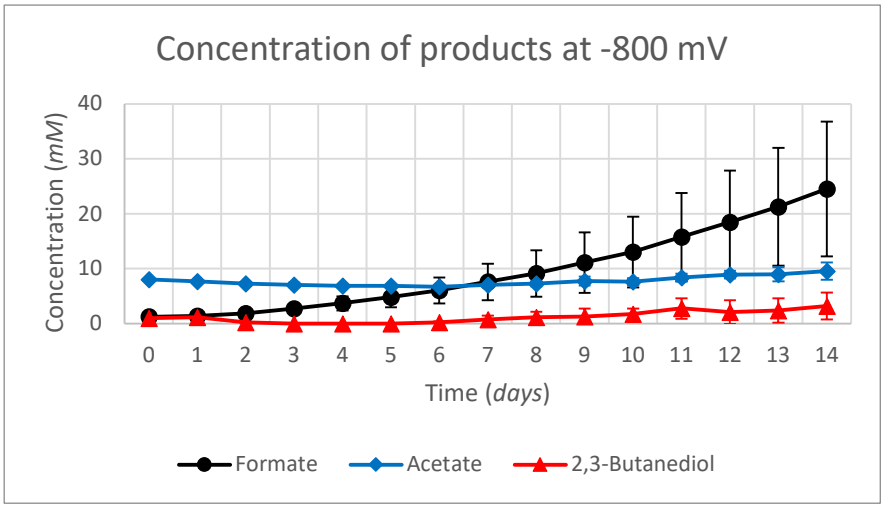

Figure 14. The average concentrations of the detected products formate, acetate and 2,3-butanediol at -800 mV during a time span of 14 days.

In the reactors with -1000 mV the products acetate, formate, 2,3-butanediol and lactate were detected. Figure 15 shows how the average concentrations of the reproducible products acetate and formate varies with time. The acetate concentration started at 6.89 mM and increased to 16.12 mM. The formate concentration, on the other hand, started at 1.39 mM but ended at 15.62 mM. The error bars demonstrate high variability among the reactors. The 2,3-butanediol and lactate could not be reproduced but were detected in respective reactor. Their

All the products increased in concentration from day 0 to day 14 except 2,3-butanediol, which did increase from 0 mM to 2.62 mM but ended up at 0 mM. Formate, acetate and lactate increased with 14.23, 9.23 and 0.55 mM, respectively, during the 14 days' time span. Further on, 2,3-butanediol and lactate were only detected in one reactor each.

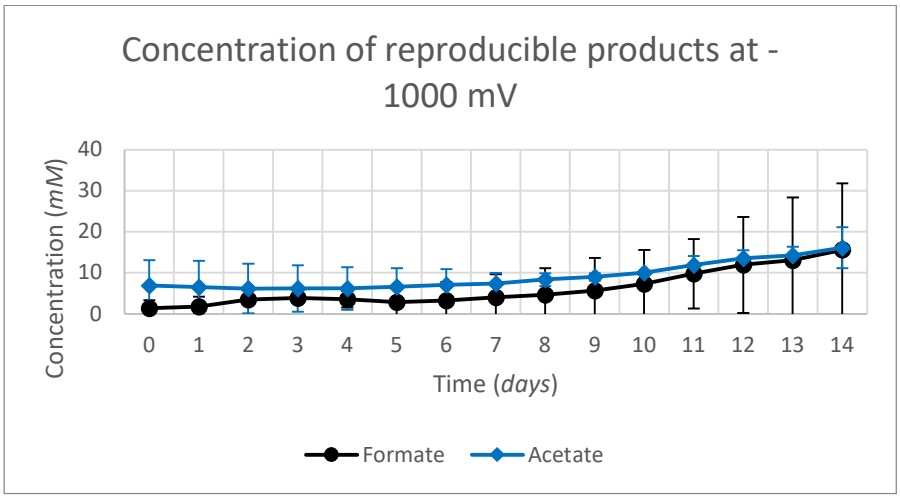

Figure 15. The average concentrations of the detected reproducible products formate and acetate at -1000 mV during a time span of 14 days.

The 2,3-butanediol and lactate could not be reproduced but were detected in respective reactor. As can be seen in figure 16, the lactate concentration increased from 11.67 mM to 12.76 mM. The 2,3-butanediol concentration on the other hand increased from 0 mM to 3.69 mM on day 12 but decreased to 0 mM again.

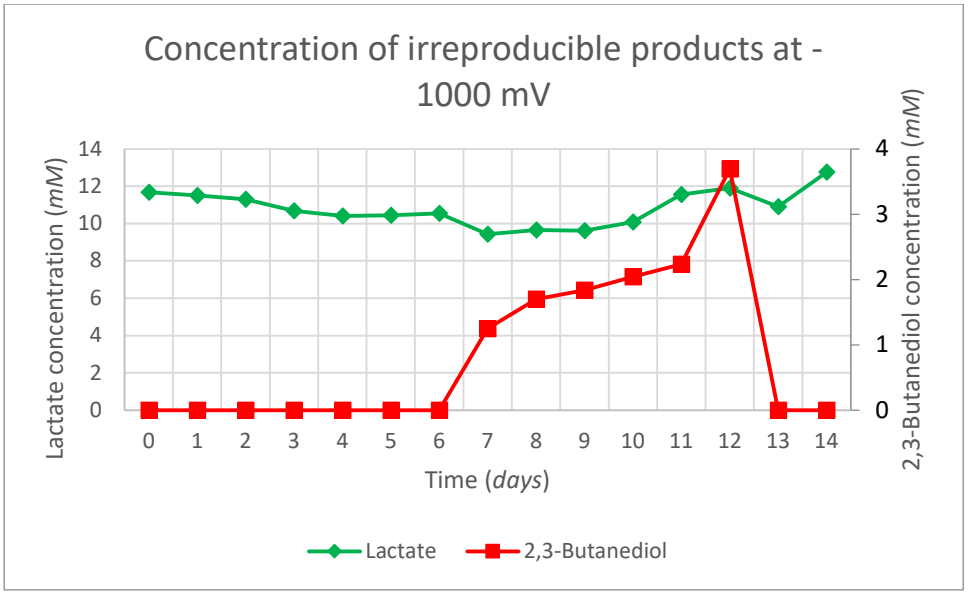

Figure 16. The average concentrations of the detected irreproducible products lactate and 2,3-butanediol at -1000 mV during a time span of 14 days.

The products acetate, formate and lactate were also detected in the anode chambers. This can be seen in figure 17 which gives an overview of the end concentration of each product for each potential. The respective concentrations in the cathode and the anode for each potential are compared at the same time as the total concentration. It can be noted that the concentrations of formate in the anode chamber at -800 mV and -1000 mV, and the concentration of lactate in the anode chamber at -1000 mV were higher than respective concentrations in the respective cathode chambers.

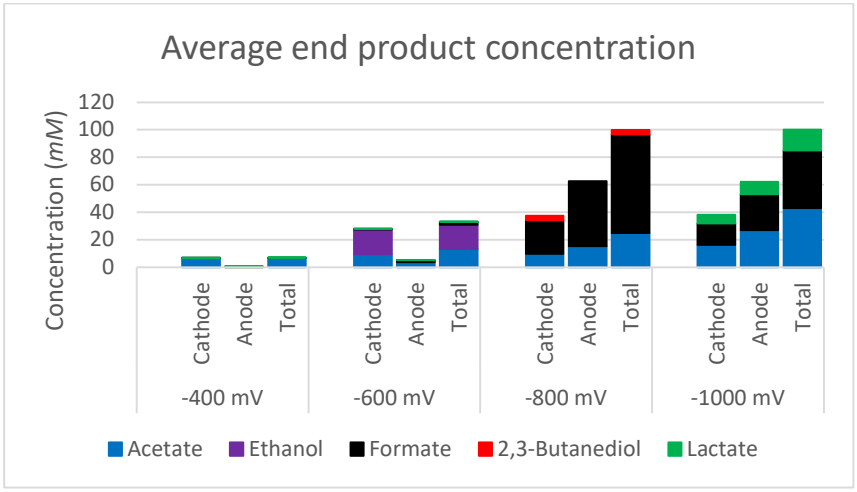

Figure 17. Average end concentrations of the products acetate, ethanol, formate, 2,3-butanediol and lactate in the cathode chamber at the potentials -400 mV, -600 mV, -800 mV and -1000 mV. The total average concentration for both the anode chamber and the cathode chamber is also shown for each potential.

3.1.2 Coulombic efficiency

In contrast to the end concentrations shown in figure 17, calculations of the coulombic efficiency were based on the concentration difference between the concentration on day 0 and day 14. Meaning that products in the cathode chamber that had negative concentration differences were excluded. Regarding the anode, only the start concentration of acetate was known because it was added to the medium, the others were assumed to be 0. The -600 mV reactors show the highest coulombic efficiencies followed by the -400 mV reactors, -1000 mV reactors and -800 mV reactors, respectively. This can be seen in figure 18.

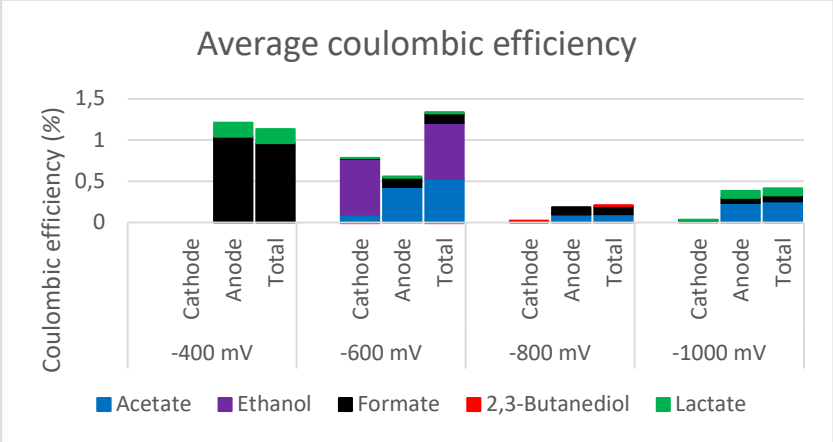

Figure 18. The average coulombic efficiency for reactors at -400 mV, -600 mV, -800 mV, and -1000 mV. The average coulombic efficiency for each product at both the cathode and anode chamber as well as the total combined is shown for each potential.

3.1.3 pH

The pH for the potentials -400 and -600 mV showed the least variance. Their respective values at day 0 were 5.10 and 5.13, respectively. On day 14, their values ended at 4.87 and 5.00, respectively. The pH for the potential -800 mV started at 5.98 and decreased to reach a value of pH 5. For -1000 mV the pH started at 5.22 and increased to 5.74 on day 3 before it decreased to 4.31 on day 14. The relationship between the average pH and time for each potential can be seen in figure 19.

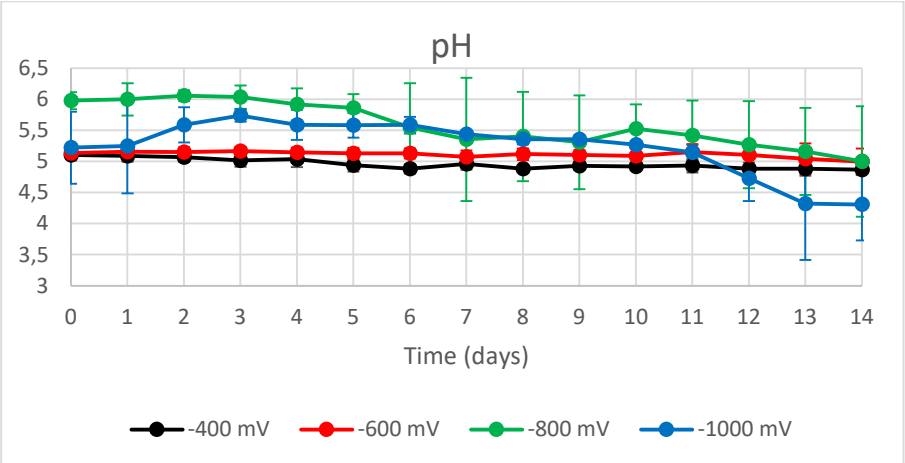

Figure 19. The average pH profile for the potentials -400, -600, -800 and -1000 mV during a time span of 14 days.

3.1.3 Cyclic voltammetry

The result from the cyclic voltammetry shows that oxidation reactions are taking place at anodic peak potentials between -534 and -600 mV vs Ag/AgCl. The anodic peak potentials can be seen in table 4.

Table 4. Peak potentials during cyclic voltammetry after operating the bio-electrochemical systems at the working potentials -400, -600, -800 and-1000 mV.

Working potential (*mV*)	**Anodic peak potential (*mV vs Ag/AgCl*)**
-400	-600
-600	-534
-800	-568
-1000	-562

3.2 Abiotic bio-electrochemical system

The product formation, coulombic efficiency and the pH for the abiotic bio-electrochemical system experiments can be found in this chapter. Supplied charge data can be found in appendix A4.

3.2.1 Product formation

In the reactors at the potential -400 mV, acetate and formate were detected. Their concentration profiles can be seen in figure 20. Acetate can be seen increasing from a concentration of 6.66 mM at day 0 to a concentration of 6.89 mM at day 14. Formate on the other hand has an average concentration of 1.09 mM at day 0 and increases to 1.12 mM at day 13, before decreasing to 0.72 mM at day 14.

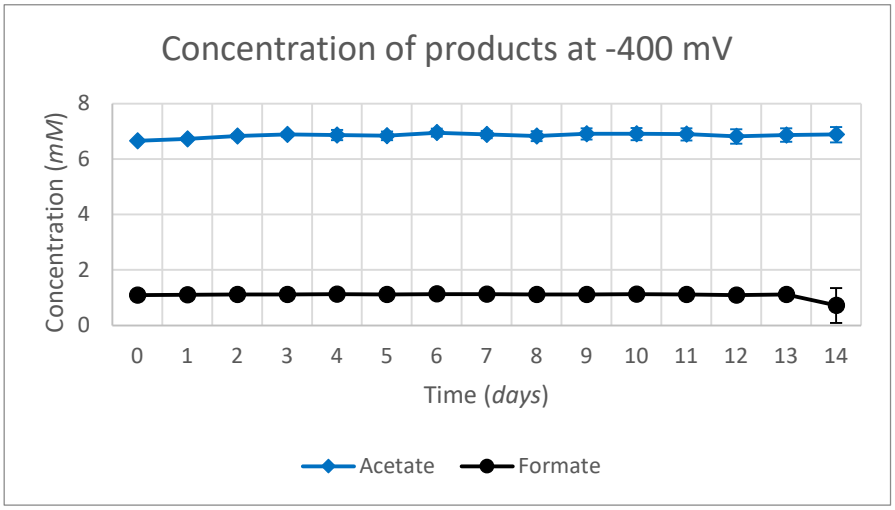

Figure 20. The average concentrations of the detected products acetate and formate at -400 mV during a time span of 14 days in an abiotic bio-electrochemical system.

Except acetate and formate, lactate was also detected in the reactors at -600 mV. It can be seen in figure 21 that an average concentration of 0.26 mM lactate was detected at day 12. Formate and acetate were detected on all days through the experiment. Formate had an average concentration of 0.37 mM on day 0 and increased to 4.44 mM on day 14. The average acetate concentration also increased from day 0 to day 14, from 7.05 to 7.93 mM.

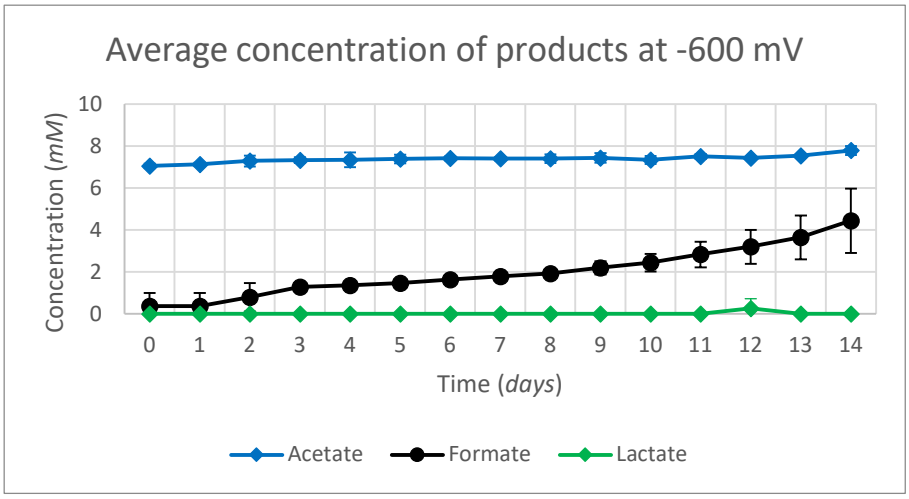

Figure 21. The average concentrations of the detected products acetate, formate and lactate at -600 mV during a time span of 14 days in an abiotic bio-electrochemical system.

Acetate, formate and lactate were also detected in the reactors at -800 mV. Figure 22 shows that lactate was only detected at days 5 to 11, where it was first detected at 0.27 mM, increased to 0.65 mM on day 8, and lastly detected at 0.30 mM. Acetate and formate were both detected on all days, and both increased in concentrations. Acetate was detected at an average concentration of 6.73 on day 0 and increased to 14.55 on day 14. Formate showed an average concentration of 0.60 mM on day 0 and increased to 33 mM on day 14. Formate also showed higher variability in concentration with higher concentrations.

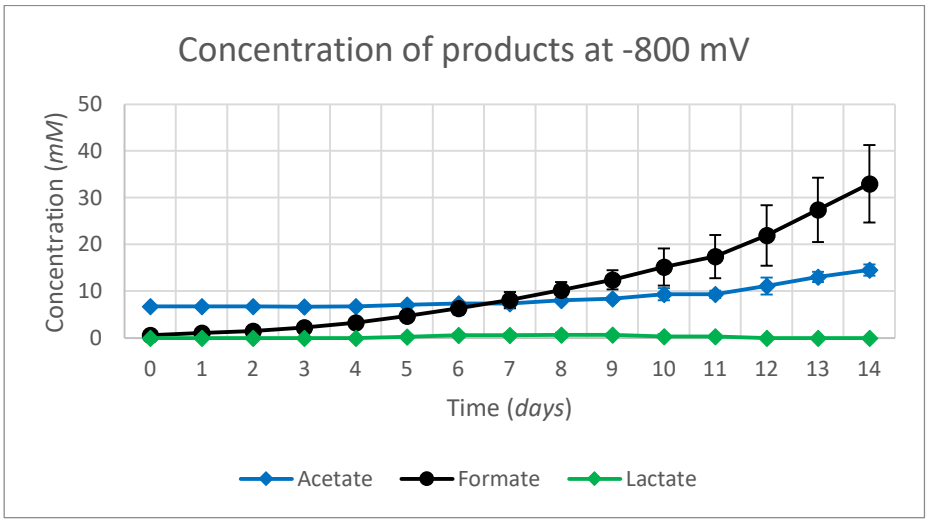

Figure 22. The average concentrations of the detected products acetate, formate and lactate at -800 mV during a time span of 14 days in an abiotic bio-electrochemical system.

Only acetate and formate were detected in the reactors at -1000 mV. Acetate was detected at an average concentration of 6.41 mM on day 0, and increased to 14.21 mM. Formate was detected at an average concentration of 1.05 mM on day 0 and increased to 47.60 mM. However, figure 23 shows high error bars for formate which testify of a high variability in formate concentration.

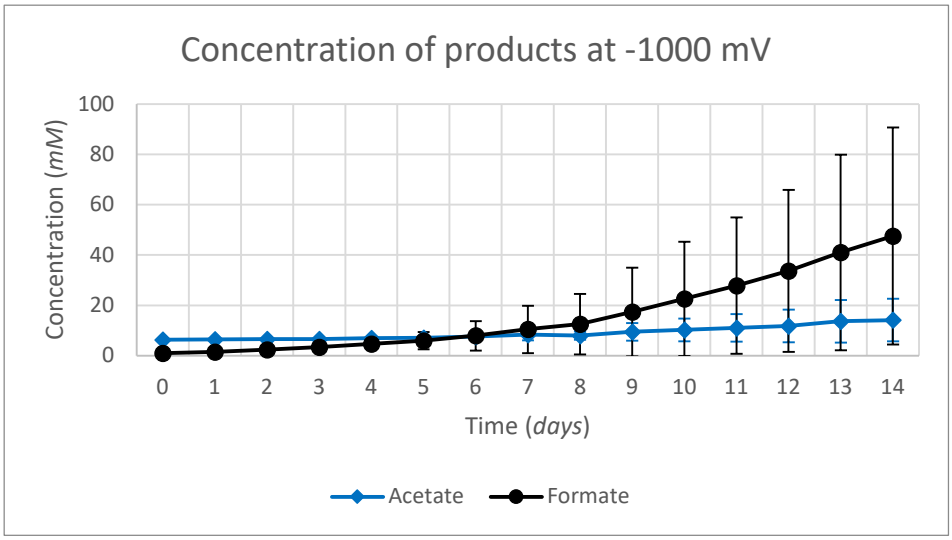

Figure 23. The average concentrations of the detected products acetate and formate at -1000 mV during a time span of 14 days in an abiotic bio-electrochemical system.

The detetcted products acetate, formate and lactate were also detected in the anode chambers of the reactors on day 14. Figure 24 shows that the final concentrations of the products acetate and formate increase for each more reductive potential. Also, there are more acetate and formate in the anode than in the cathode chamber for each potential, except at -400 mV.

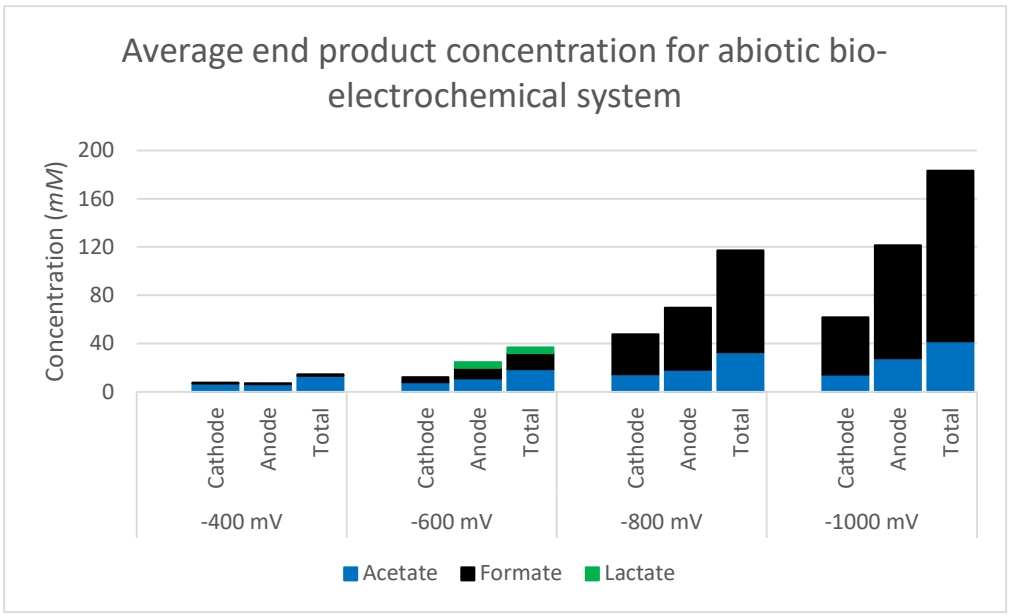

Figure 24. Average end concentrations of the products acetate, formate and lactate in the cathode and anode chambers at the potentials -400 mV, -600 mV, -800 mV and -1000 mV. The total average concentration for both the anode chamber and the cathode chamber is also shown for each potential.

3.2.2 Coulombic efficiency

In contrast to the end concentrations shown in figure 24, the calculations of the coulombic efficiency were based on the concentration difference between the concentration on day 0 and day 14. Meaning that products in the cathode chamber that had negative concentration differences were excluded. Regarding the anode, only the start concentration of acetate was known, the others were assumed to be 0. The coulombic efficiency for the for acetate in the anode chamber at -400 mV was approximately 33 percent because a low charge in comparison to the other potentials was used. The coulombic efficiency for acetate in the -400 mV is shown in figure 25.

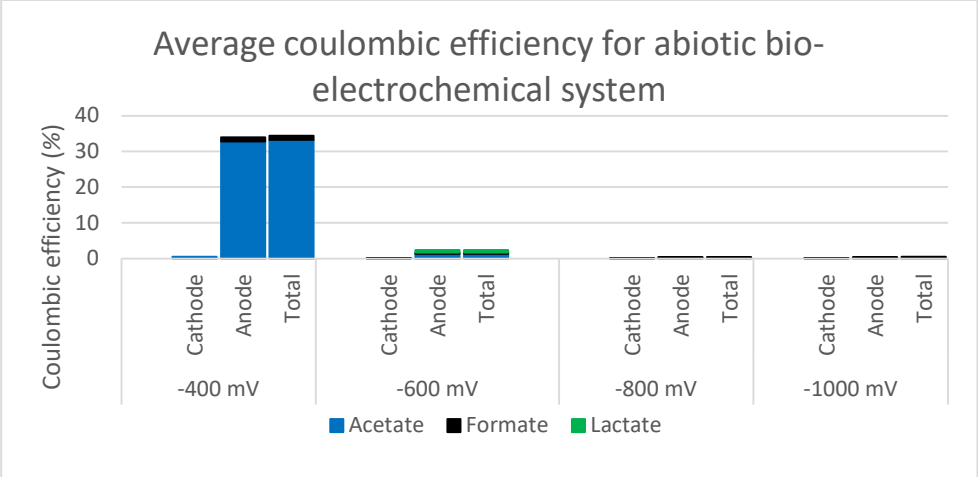

Figure 25. The average coulombic efficiency for reactors at -400 mV, -600 mV, -800 mV, and -1000 mV. The average coulombic efficiency for each product at both the cathode and anode chamber as well as the total combined is shown for each potential.

Other coulombic efficiencies for the produced products in the reactors at -600, -800 and -1000 mV were approximately 2.3 percent, 0.4 percent, and 0.4 percent, respectively. This is seen in figure 26 where acetate in the anode of the -400 mV reactors is excluded.

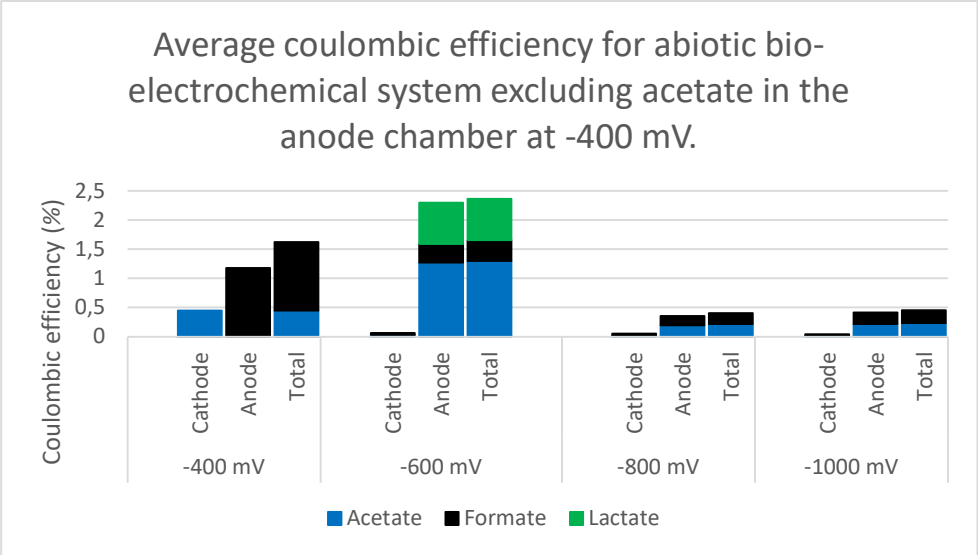

Figure 26. The average coulombic efficiency for reactors at -400 mV, -600 mV, -800 mV, and -1000 mV. The average coulombic efficiency for each product at both the cathode and anode chamber as well as the total combined is shown for each potential, except for acetate in the anode chamber at -400 mV.

3.2.3 pH

The average pH profiles for the potentials -400, -600, -800 and -1000 mV can be seen in figure 25. The average pH for the -400 mV reactors starts at a value of pH 4.76 and decreases to pH 4.45 on day 14. The average pH of the -600 mV and -800 mV reactors start at 5.10 and 5.19, and increases to 5.36 and 5.78 on day 2, respectively. After day 2, the average pH decreases to 4.80 and 5.27, respectively. The average pH of the reactors at -1000 mV starts at 5.67 on day 0 and ends at 4.65 on day 14. The pH value at -1000 mV shows high variability and fluctuates up and down.

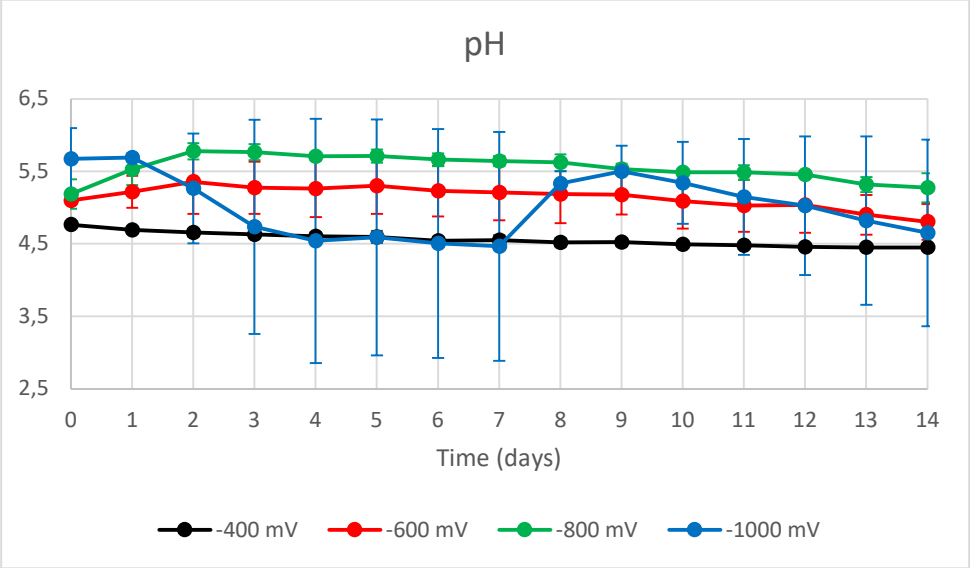

Figure 27. The average pH profile for the potentials -400, -600, -800 and -1000 mV in abiotic conditions during a time span of 14 days.

3.2.4 Cyclic voltammetry

The result from the cyclic voltammetry shows that oxidation reactions are taking place at anodic peak potentials between -589 and -617 mV vs Ag/AgCl. The anodic peak potentials can be seen in table 5.

Table 5. Peak potentials during cyclic voltammetry after operating the bio-electrochemical systems at the working potentials -400, -600, -800 and-1000 mV.

Working potential (*mV*)	**Anodic peak potential (*mV vs Ag/AgCl*)**
-400	-617
-600	-614
-800	-589
-1000	-600

3.3 Serum flask control experiments

The product formation, pH and growth profiles for the serum flask control experiments can be found in this chapter.

3.3.1 Product formation

The detected products in the serum flasks with the conditions pH 5.7 and 2 bar 80:20 H_2:CO_2 gas were acetate, formate and 2,3-butanediol. Their concentration profiles can be seen in figure 28. 2,3-butanediol was detected at a concentration of 1.39 mM on day 0, which increased to 1.51 mM on day 1 before decreasing to 0 mM on day 7. The concentrations of acetate and formate both increased during the time span. The average acetate concentration increased from 5.11 mM on day 0 to 55.07 on day 14. Formate was first detected at an average concentration of 1.70 on day 0 and increased to 11.30 mM on day 8. Then it decreased 10.08 mM.

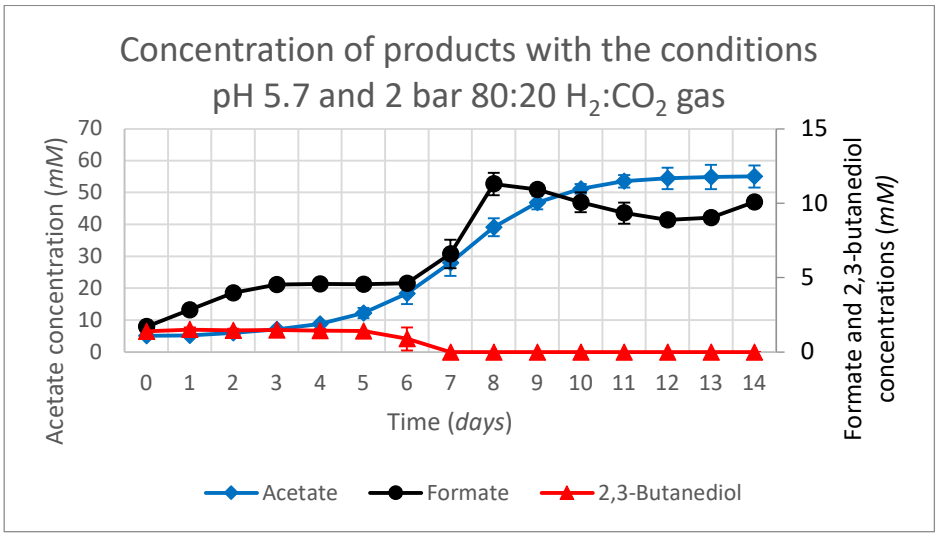

Figure 28. The average concentrations of the detected products acetate, formate and 2,3-butanediol in serum flasks with the conditions pH 5.7 and 2 bar 80:20 H_2:CO_2 gas during a time span of 14 days.

In the serum flasks with the conditions pH 5.0 and 2 bar 80:20 H_2:CO_2 gas, the products acetate, formate and ethanol were detected. Figure 29 shows that during the time span of 14 days, the average concentration of acetate increases from 10.07 mM to 80.28 mM. Formate is first detected on day 1 with an average concentration of 2.70 mM. It then decreases to 0 mM on day 10. Ethanol is first detected on day 11, and its average concentration increases to 13.86 mM on day 14.

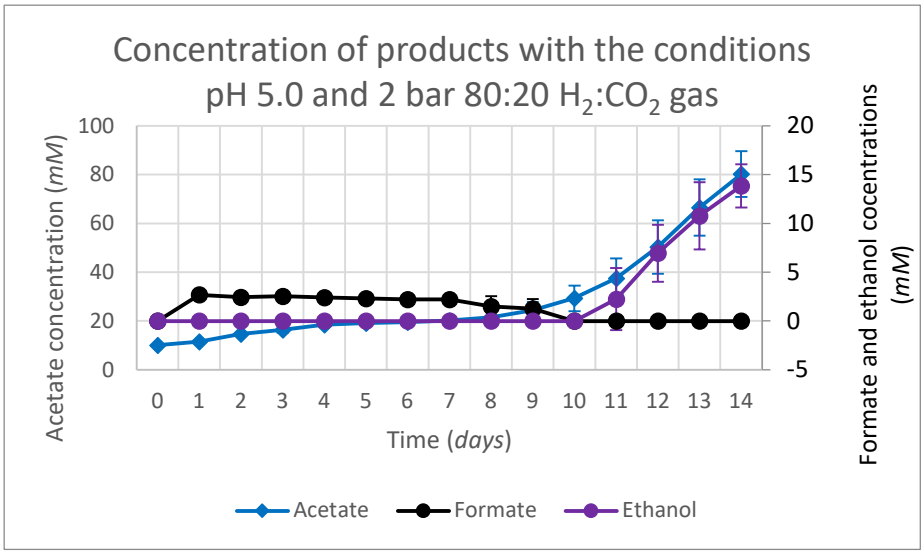

Figure 29. The average concentrations of the detected products acetate, formate and ethanol in serum flasks with the conditions pH 5.0 and 2 bar 80:20 H_2:CO_2 gas during a time span of 14 days.

Acetate, formate and 2,3-butanediol were detected in the serum flasks with the conditions pH 5.7 and 1 bar 99.99 percent CO_2 gas. Figure 30 shows the average concentration profile of these product during the time span of 14 days. Acetate was detected on day 0 with an average concentration of 6.38 mM. It then increased to 7.37 mM on day 14. Formate was also detected on day 0, but with an average concentration of 1.11 mM. It then decreased to 0 mM on day 6 and was not detected again. 2,3-butanediol was on the other hand detected every day. It had an average concentration of 0.97 mM on day 0 and increased to 2.18 mM on day 14.

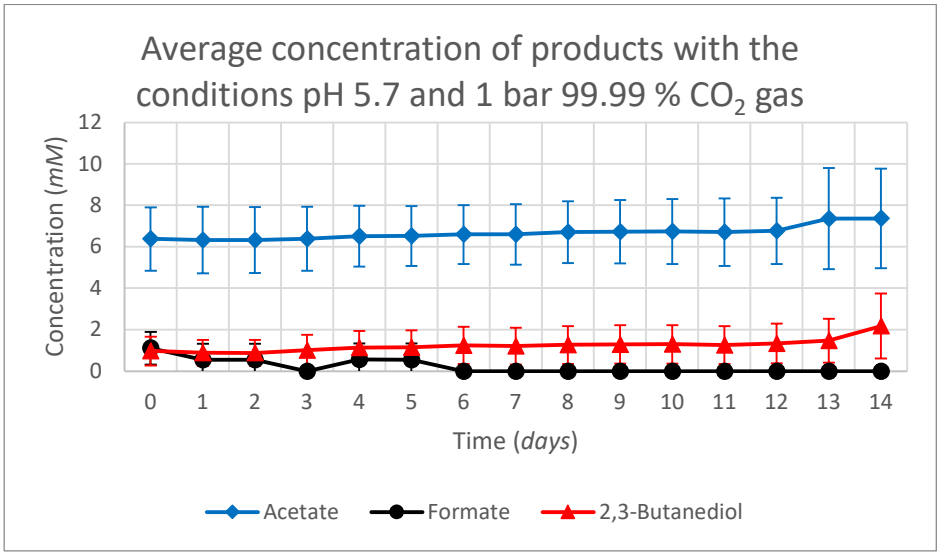

Figure 30. The average concentrations of the detected products acetate, formate and 2,3-butanediol in serum flasks with the conditions pH 5.7 and 1 bar 99 percent CO_2 gas during a time span of 14 days.

Only formate and acetate were detected in the serum flasks with the conditions pH 5.0, 80:20 H_2:CO_2 gas, and 50 mM formic acid. Acetate was detected on day 0 with an average concentration of 14.75 mM, which increased to 14.92 mM on day 14. The average formate concentration decreased from 74.24 mM to 71.47 mM from day 0 to day 14. However, both

the average acetate and formate concentrations dropped to 9.98 and 47.58 mM, respectively, on day 12. The concentration profiles of acetate and formate can be seen in figure 31.

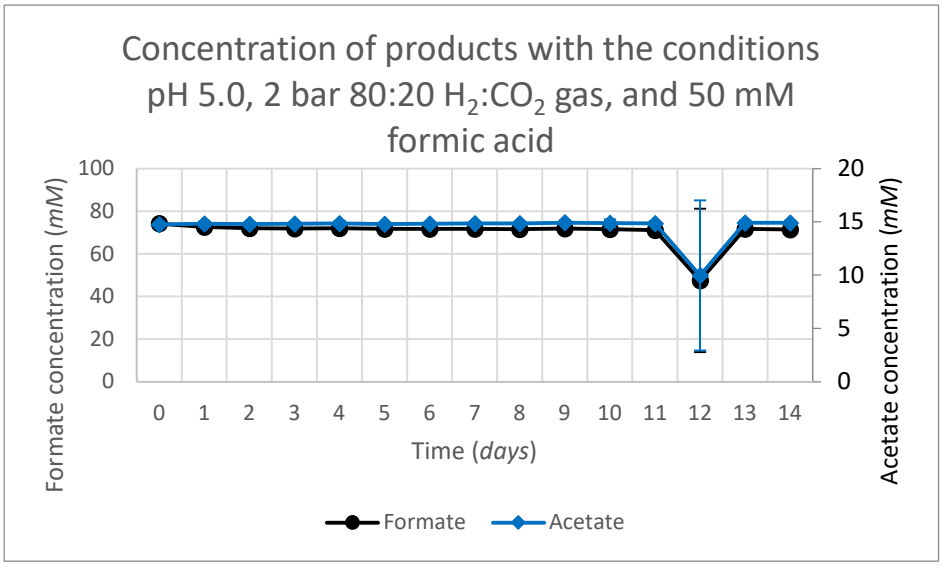

Figure 31. The average concentrations of the detected products acetate and formate in serum flasks with the conditions pH 5.0 and 2 bar 80:20 H_2:CO_2 gas, and 50 mM formic acid during a time span of 14 days.

3.3.1 pH and growth profiles

For the serum flasks with the conditions pH 5.7 and 2 bar 80:20 H_2:CO_2 gas, it can be seen that *C. ljungdahlii* is growing from an optical density of 0.03 on day 0 to and optical density of 0.653 on day 10. The optical density then decreases. The corresponding pH starts at a value of 5.67 on day 0 and decreases to 4.74 on day 10, before it stabilizes. The serum flasks with the conditions pH 5.0 and 2 bar 80:20 H_2:CO_2 gas also show an increase in optical density, starting at 0.031 on day 0 and increasing to 0.585 on day 14. The corresponding pH is seen decreasing from a value of 5.04 on day 0 to pH 4.21 on day 14.

In the serum flasks with the conditions pH 5.7 and 1 bar 99.99 percent CO_2 gas, the optical density decreased from 0.026 to 0.020 from day 0 to day 14. The corresponding pH increases from 5.61 to 5.62 during the same period. Lastly, in the serum flasks with the conditions pH 5.0, 80:20 H_2:CO_2 gas, and 50 mM formic acid, the optical density decreased from 0.033 to 0.021. The pH decreased from 5.16 to 5.15. Figure 32 displays the pH and growth profiles for the conditions used in the serum flask control experiments.

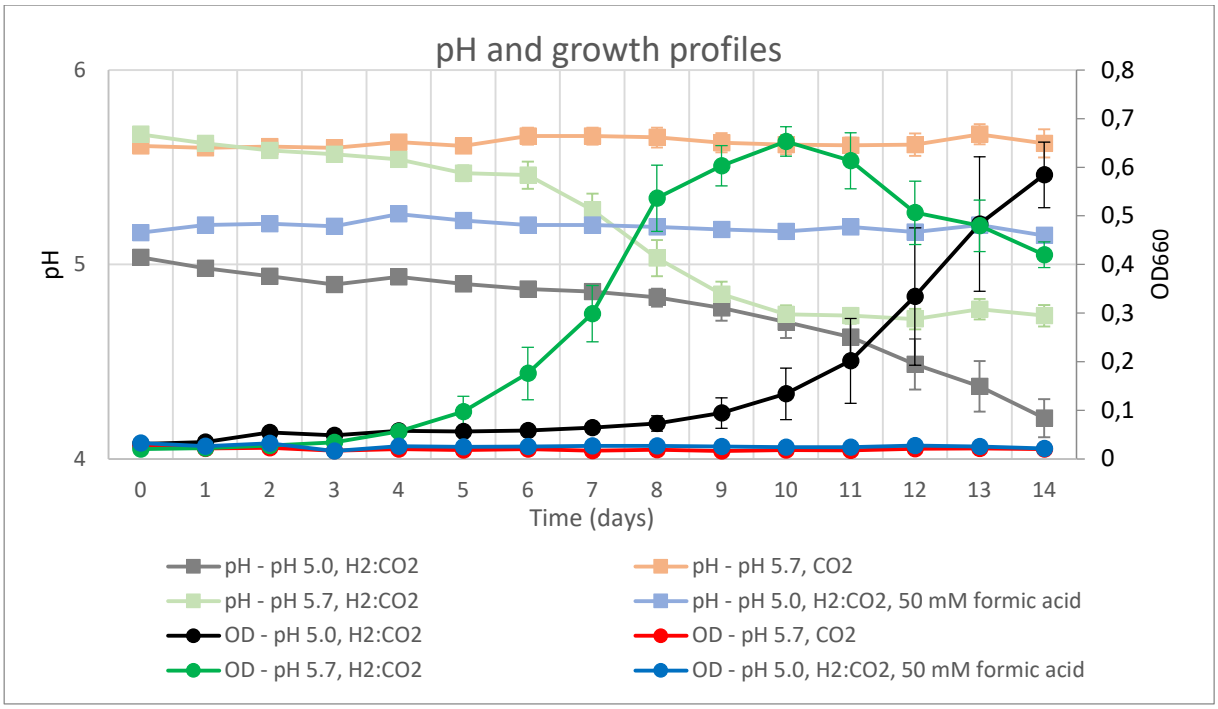

Figure 32. pH and growth profiles for the serum flask control experiments with the conditions: pH 5.7, 2 bar 80:20 H_2:CO_2 gas; pH 5.0 and 2 bar 80:20 H_2:CO_2 gas; pH 5.7 and 1 bar 99.99 percent CO_2 gas; pH 5.0, 80:20 H_2:CO_2 gas, and 50 mM formic acid. OD_{660} is optical density at a wavelength of 660 nm.

4. Discussion

4.1 Comparison of the product formations between the biotic and abiotic experiments

4.1.1 Bio-electrochemical systems at -400 mV

Comparing the product formation in the biotic bio-electrochemical system reactors with their abiotic counterpart at the potential -400 mV, acetate and formate were detected in the reactors with both conditions. The overall acetate concentration is higher in the biotic reactors but is decreasing slightly compared to the abiotic reactors. The higher acetate concentration could be due to the inoculum media also containing some acetate itself. Because as seen in the serum flask control experiment with the same conditions as the preculture, *C. ljungdahlii* was producing acetate. The decrease in acetate concentration could be due to acetate diffusing over the membrane to the anode chamber, where it would be a lower concentration of acetate. The decrease could also be because the cells consume some of the acetate.

Formate, which has a constantly higher concentration in the abiotic reactor, can be formed both inside the cells and in the electrolyte. The fact that the formate concentration is decreasing in the biotic reactor could be due to the cells consuming it in the Wood-Ljungdahl pathway. And when the formate has been used up the potential is too low for sufficient formate to be reproduced so the concentration doesn't increase again. The very low amount of 2,3-butanediol and lactate, that are only detected in the biotic reactors, both vary up and down in concentration. Lactate was not detected in any of the serum flask control experiments while 2,3-butanediol was seen increasing when there was no H_2 gas available. So, 2,3-butanediol production might be produced because the cells are stressed.

4.1.2 Bio-electrochemical systems at -600 mV

At -600 mV, acetate is detected in both the abiotic and biotic reactors. Their concentrations are increasing in a similar manner and approximately the same amount, even though the start concentration in the biotic reactor is a bit higher. Probably because it was already produced by the inoculum. Formate is also detected in both the biotic and abiotic reactors but the concentrations in the abiotic are significantly higher and is increasing clearly throughout the period. The lower concentration of formate in the biotic reactors could again be because *C. ljungdahlii* is consuming it.

2,3-butanediol is only detected in the biotic reactors which could mean that the *C. ljungdahlii* cells must have produced it. And even though it was in only one reactor, ethanol was also only detected in the biotic experiment. The ethanol production would be consistent with the ethanol production in the serum flask with pH 5.0 and 2 bar 80:20 H_2:CO_2 gas. Another product that could not be detected in more than one biotic reactor was lactate, where it can be seen already detected on day 0 and then increasing to 0.15 mM. Lactate is also detected in the abiotic reactors, but only once on day 12 and in a concentration of 0.26 mM.

4.1.3 Bio-electrochemical systems at -600 mV

At -800 mV acetate is again detected in both the biotic and abiotic reactors and the concentration profiles are like the acetate concentrations at -600 mV. But at -800 mV the acetate concentration is increasing more in the abiotic reactors. A reason for the lower acetate concentrations in the biotic reactors could be due to the 2,3-butanediol production. 2,3-butanediol is only detected in the biotic reactors and it is seen increasing in concentration. The 2,3-butanediol production could also be a reason why the formate concentration is lower in the biotic reactors than in the abiotic. Finally, lactate is only detected in the abiotic reactors and a reason for this could be that it has been produced in the anodic chamber and then diffused over the membrane. Because lactic acid has been produced abiotically (Dai et al., 2017).

4.1.4 Bio-electrochemical systems at -1000 mV

At -1000 mV, formate and acetate are the only detected products in the abiotic reactors. Formate is detected in higher concentrations in the abiotic reactors than in the biotic reactors while the acetate concentrations are similar. Also in the biotic reactors are lactate and 2,3-butanediol detected. But they are detected in only one reactor each and couldn't be reproduced. Lactate is detected at a concentration of 11.7 mM on day 0 and it stays in that magnitude, and 2,3-butanediol increases to a concentration of 3.7 mM before disappearing. These are the highest concentration lactate and 2,3-butanediol are detected at and they weren't produced simultaneously. Which means that if they were produced by *C. ljungdahlii* because levels of reducing equivalents needed to be decreased, only one metabolic pathway was used at a time. Maybe because it is more energy efficient to use less enzymes.

4.2 Comparison of the potentials

4.2.1 Product formation

One pattern that can be seen between the different potentials is that more formate is produced when the potential is more negative. This is specifically visible in the abiotic bio-electrochemical system. For the biotic bio-electrochemical system, more formate was detected at -800 mV than -1000 mV. Another product that is seen more of by having a more negative potential is lactate. Though not reproducible at -600 and -1000 mV, it was shown to increase in the biotic bio-electrochemical system. For acetate, an increase was seen in concentration from -400 mV to -1000 mV, but depending on if the reactor was biotic or abiotic, there was no significant difference between -600 and -800, and -800 and -1000 mV, respectively. But 2,3-butanediol which was reproducible at the potentials -400, -600 and -800 mV showed a steady increase in concentration with more negative potentials. This pattern would have been repeated for the -1000 mV if the 2,3-butanediol would have been reproduced. One potential that stood out was -600 mV because ethanol was only detected at that potential, though not reproducible.

4.2.2 pH

Regarding the pH it is constant throughout the experiment for the -400 mV. At -400 mV, there was no significant acetate or formate production either production either. The pH for the biotic -600 mV reactors is also constant. While the pH for the other potentials is increasing initially and then decreasing. The pH rise could be due to electrons from the

current reacting with protons in the medium. Then when there is more acetate produced, there are not sufficient electrons to balance the decreasing pH.

4.2.3 Coulombic efficiency

The coulombic efficiency is very low except for the acetate detected in the anode chamber of the abiotic reactors at -400 mV. The coulombic efficiency for a product should indicate about how large proportion of the supplied coulombs were consumed and accumulated in that product. But there could not be any acetate produced in the abiotic reactor. If there was a contamination in one reactor, then there would be contaminations in all the abiotic reactors at -400 mV. A solution to have a better understanding of how the acetate concentration varied could have been to take samples from the anode chamber as well every 24 hours.

Formate concentrations which increased with more negative potentials and maybe should have shown higher coulombic efficiencies, did not. This because the supplied current increased more than what the formate concentrations did for the different potentials. One could speculate that the rest of the current went to production of for example H_2 gas or growth of the cells, and there could have been a lot of H_2 gas being evolved but it wasn't measured. The growth on the other hand which was measured with optical density showed only a decline in all reactors at all potentials. Growth profile data is seen in appendix A3.

4.3 Comparison of cyclic voltammetry results

When comparing the peak potentials between the different working potentials, there is no pattern to describe as the peak potentials vary too much. However, when comparing biotic and abiotic bio-electrochemical systems, there is a slight difference between biotic and abiotic conditions at all working potentials. The peak potentials are more negative in the abiotic reactors. And the only difference between the biotic and abiotic reactors are the inoculated cells, which means that the cells must have secreted something that is oxidated in the medium. But the known products that are produced by the cells have less negative oxidation potentials (Li et al., 2018) and they can't be the cause of the peaks. Also, regardless of what causes the peaks, it is still hard to argue for what chemical species could cause the difference between biotic and abiotic conditions when there is no specific pattern between the working potentials.

4.4 Future improvements

If this experiment would be repeated, one thing that could be changed would be to lower the formate concentrations in the serum flask control experiments. The formate concentration in the control serum flask which would contain 50 mM got up to 80 mM, which was too poisonous for *C. ljungdahlii*. 50 mM was chosen because concentrations up to 40 mM was detected in the biotic bio-electrochemical system. But the concentrations of 10, 20, 30 and 40 mM could be set so that the poisonous effect could be avoided. Furthermore, it would give a better understanding of the product formation if sampling could also be done in the anode chamber of the bio-electrochemical system reactors. Because then a better overview could be obtained of how different product concentrations vary in the whole system. It would also give a better basis for calculation the coulombic efficiencies of the different products.

5. Conclusions

From the results of this report where the bio-electrochemical activity of *C. ljungdahlii* was to be investigated at the potentials of -400 mV, -600 mV, -800 mV and -1000 mV several conclusions can be drawn. It can be concluded that *C. ljungdahlii* can produce 2,3-butanediol with an increasing production up to -800 mV in a bio-electrochemical system. It can also be concluded that when *C. ljungdahlii* is inoculated into the bio-electrochemical system there is a smaller formate concentration in the electrolyte. Suggesting that formate is used by *C. ljungdahlii*. Furthermore, the coulombic efficiencies are very low, suggesting that the electron uptake is limited.

6. Reference list

Allen J. Bard, L. R. F. (2001). Electrochemical Methods: Fundamentals and Applications. In *JOHN WILEY & SONS, INC* (Issue 2). http://elib.tu-darmstadt.de/tocs/95069577.pdf

Badwal, S. P. S., Giddey, S. S., Munnings, C., Bhatt, A. I., & Hollenkamp, A. F. (2014). Emerging electrochemical energy conversion and storage technologies. *Frontiers in Chemistry*, *2*(SEP). https://doi.org/10.3389/fchem.2014.00079

Bajracharya, S. (2016). *Microbial electrosynthesis of biochemicals*.

Barbosa, S. G., Peixoto, L., Alves, J. I., & Alves, M. M. (2021). Bioelectrochemical systems (BESs) towards conversion of carbon monoxide/syngas: A mini-review. *Renewable and Sustainable Energy Reviews*, *135*(January 2020). https://doi.org/10.1016/j.rser.2020.110358

Britannica. (2021). *biofuel | Definition, Types, & Pros and Cons*. https://www.britannica.com/technology/biofuel

Choudhary, M., Joshi, S., Singh, P., & Srivastava, N. (2020). Biofuel production from lignocellulosic biomass: Introduction and metabolic engineering for fermentation scale-up. *Genetic and Metabolic Engineering for Improved Biofuel Production from Lignocellulosic Biomass*, 1–12. https://doi.org/10.1016/B978-0-12-817953-6.00001-4

Dai, C., Sun, L., Liao, H., Khezri, B., Webster, R. D., Fisher, A. C., & Xu, Z. J. (2017). Electrochemical production of lactic acid from glycerol oxidation catalyzed by AuPt nanoparticles. *Journal of Catalysis*, *356*, 14–21. https://doi.org/10.1016/j.jcat.2017.10.010

Elgrishi, N., Rountree, K. J., McCarthy, B. D., Rountree, E. S., Eisenhart, T. T., & Dempsey, J. L. (2018). A Practical Beginner's Guide to Cyclic Voltammetry. *Journal of Chemical Education*, *95*(2), 197–206. https://doi.org/10.1021/acs.jchemed.7b00361

Harnisch, F., & Freguia, S. (2012). A basic tutorial on cyclic voltammetry for the investigation of electroactive microbial biofilms. *Chemistry - An Asian Journal*, *7*(3), 466–475. https://doi.org/10.1002/asia.201100740

Hermann, M., Teleki, A., Weitz, S., Niess, A., Freund, A., Bengelsdorf, F. R., Dürre, P., & Takors, R. (2021). Identifying and Engineering Bottlenecks of Autotrophic Isobutanol Formation in Recombinant C. ljungdahlii by Systemic Analysis. *Frontiers in Bioengineering and Biotechnology*, *9*(March), 1–14. https://doi.org/10.3389/fbioe.2021.647853

Im, C. H., Song, Y. E., Jeon, B. H., & Kim, J. R. (2016). Biologically activated graphite fiber electrode for autotrophic acetate production from CO2 in a bioelectrochemical system. *Carbon Letters*, *20*(1), 76–80. https://doi.org/10.5714/CL.2016.20.076

Jiang, Y., May, H. D., Lu, L., Liang, P., Huang, X., & Ren, Z. J. (2019). Carbon dioxide and organic waste valorization by microbial electrosynthesis and electro-fermentation. *Water Research*, *149*, 42–55. https://doi.org/10.1016/j.watres.2018.10.092

Karthikeyan, R., Singh, R., & Bose, A. (2019). Microbial electron uptake in microbial

electrosynthesis: a mini-review. *Journal of Industrial Microbiology and Biotechnology*, *46*(9–10), 1419–1426. https://doi.org/10.1007/s10295-019-02166-6

Köpke, M., Mihalcea, C., Liew, F. M., Tizard, J. H., Ali, M. S., Conolly, J. J., Al-Sinawi, B., & Simpson, S. D. (2011). 2,3-Butanediol production by acetogenic bacteria, an alternative route to chemical synthesis, using industrial waste gas. *Applied and Environmental Microbiology*, *77*(15), 5467–5475. https://doi.org/10.1128/AEM.00355-11

Li, Y., Xu, D., Chen, C., Li, X., Jia, R., Zhang, D., Sand, W., Wang, F., & Gu, T. (2018). Anaerobic microbiologically influenced corrosion mechanisms interpreted using bioenergetics and bioelectrochemistry: A review. *Journal of Materials Science and Technology*, *34*(10), 1713–1718. https://doi.org/10.1016/j.jmst.2018.02.023

Liew, F., Martin, M. E., Tappel, R. C., Heijstra, B. D., Mihalcea, C., & Köpke, M. (2016). Gas Fermentation-A flexible platform for commercial scale production of low-carbon-fuels and chemicals from waste and renewable feedstocks. *Frontiers in Microbiology*, *7*(MAY). https://doi.org/10.3389/fmicb.2016.00694
cited By 29

Lin, C. Y., & Lu, C. (2021). Development perspectives of promising lignocellulose feedstocks for production of advanced generation biofuels: A review. *Renewable and Sustainable Energy Reviews*, *136*. https://doi.org/10.1016/j.rser.2020.110445

Liu, Z. Y., Jia, D. C., Zhang, K. Di, Zhu, H. F., Zhang, Q., Jiang, W. H., Gu, Y., & Li, F. L. (2020). Ethanol Metabolism Dynamics in Clostridium ljungdahlii Grown on Carbon Monoxide. *Applied and Environmental Microbiology*, *86*(23), 1–14. https://doi.org/10.1128/AEM.02376-20

Marcellin, E., Behrendorff, J. B., Nagaraju, S., Detissera, S., Segovia, S., Palfreyman, R. W., Daniell, J., Licona-Cassani, C., Quek, L. E., Speight, R., Hodson, M. P., Simpson, S. D., Mitchell, W. P., Köpke, M., & Nielsen, L. K. (2016). Low carbon fuels and commodity chemicals from waste gases-systematic approach to understand energy metabolism in a model acetogen. *Green Chemistry*, *18*(10), 3020–3028. https://doi.org/10.1039/c5gc02708j

Michael Köpke, Monica L. Gerth, Danielle J. Maddock, Alexander P. Mueller, FungMin Liew, Séan D. Simpson, W. M. P. (2014). Reconstruction of an Acetogenic 2,3-Butanediol Pathway Involving aNovel NADPH-Dependent Primary-Secondary Alcohol Dehydrogenase.pdf. *Applied and Environmental Microbiology*. https://doi.org/10.1128/AEM.00301-14

NASA. (2021a). *Causes | Facts – Climate Change: Vital Signs of the Planet*. https://climate.nasa.gov/causes/

NASA. (2021b). *NASA: Climate Change and Global Warming*. https://climate.nasa.gov/

Nevin, K. P., Hensley, S. A., Franks, A. E., Summers, Z. M., Ou, J., Woodard, T. L., Snoeyenbos-West, O. L., & Lovley, D. R. (2011). Electrosynthesis of organic compounds from carbon dioxide is catalyzed by a diversity of acetogenic microorganisms. *Applied and Environmental Microbiology*, *77*(9), 2882–2886. https://doi.org/10.1128/AEM.02642-10

NOAA. (2021). *Climate Change: Atmospheric Carbon Dioxide*.

Patil, S. A., Hägerhäll, C., & Gorton, L. (2014). Electron transfer mechanisms between microorganisms and electrodes in bioelectrochemical systems. *Bioanalytical Reviews*, *1*(September 2016), 71–129. https://doi.org/10.1007/11663_2013_2

Richter, H., Molitor, B., Wei, H., Chen, W., Aristilde, L., & Angenent, L. T. (2016). Ethanol production in syngas-fermenting: Clostridium ljungdahlii is controlled by thermodynamics rather than by enzyme expression. *Energy and Environmental Science*, *9*(7), 2392–2399. https://doi.org/10.1039/c6ee01108j

Schuchmann, K., & Müller, V. (2014). Autotrophy at the thermodynamic limit of life: A model for energy conservation in acetogenic bacteria. *Nature Reviews Microbiology*, *12*(12), 809–821. https://doi.org/10.1038/nrmicro3365

Schuchmann, K., & Müller, V. (2016). Energetics and application of heterotrophy in acetogenic bacteria. *Applied and Environmental Microbiology*, *82*(14), 4056–4069. https://doi.org/10.1128/AEM.00882-16

Sun, X., Atiyeh, H. K., Huhnke, R. L., & Tanner, R. S. (2019). Syngas fermentation process development for production of biofuels and chemicals: A review. *Bioresource Technology Reports*, *7*(July), 100279. https://doi.org/10.1016/j.biteb.2019.100279

UNFCCC. (2021). *The Paris Agreement*. https://unfccc.int/process-and-meetings/the-paris-agreement/the-paris-agreement

Westerholm, M., Moestedt, J., & Schnürer, A. (2016). Biogas production through syntrophic acetate oxidation and deliberate operating strategies for improved digester performance. *Applied Energy*, *179*(October), 124–135. https://doi.org/10.1016/j.apenergy.2016.06.061

Zheng, T., Li, J., Ji, Y., Zhang, W., Fang, Y., Xin, F., Dong, W., Wei, P., Ma, J., & Jiang, M. (2020). Progress and Prospects of Bioelectrochemical Systems: Electron Transfer and Its Applications in the Microbial Metabolism. *Frontiers in Bioengineering and Biotechnology*, *8*(January), 1–10. https://doi.org/10.3389/fbioe.2020.00010

Appendix

Appendix A1 - Modified Wolin's mineral solution

Table A6. Listed components for making the modified Wolin's mineral solution.

Nitrilotriacetic acid	1.5 g
$MgSO_4 \times 7H_2O$	3 g
$MnSO_4 \times H_2O$	0.5 g
NaCl	1 g
$FeSO_4 \times 7H_2O$	0.1 g
$CoSO_4 \times 7H_2O$	0.18 g
$CaCl_2 \times 2H_2O$	0.1 g
$ZnSO_4 \times 7H_2O$	0.18 g
$CuSO_4 \times 5H_2O$	0.01 g
$KAl(SO_4)_2 \times 12H_2O$	0.02 g
H_3BO_3	0.01 g
$Na_2MoO_4 \times 2H_2O$	0.01 g
$NiCl_2 \times 6H_2O$	0.03 g
$Na_2SeO_3 \times 5H_2O$	0.3 mg
$Na_2WO_4 \times 2H_2O$	0.4 mg
Distilled water	1000 mL

Appendix A2 - Wolin's vitamin solution

Table A7. Listed components for making the Wolin's vitamin solution.

Biotin	2 mg
Folic acid	2 mg
Pyridoxine-HCl	10 mg
Thiamine-HCl	5 mg
Riboflavin	5 mg
Nicotinic acid	5 mg
Ca-D-pantothenate	5 mg
Vitamin B12	0.10 mg
p-Aminobenzoic acid	5 mg
(±)-α-Lipoic acid	5 mg
Distilled water	1000 mL

Appendix A3 – Average growth profiles for biotic bio-electrochemical system

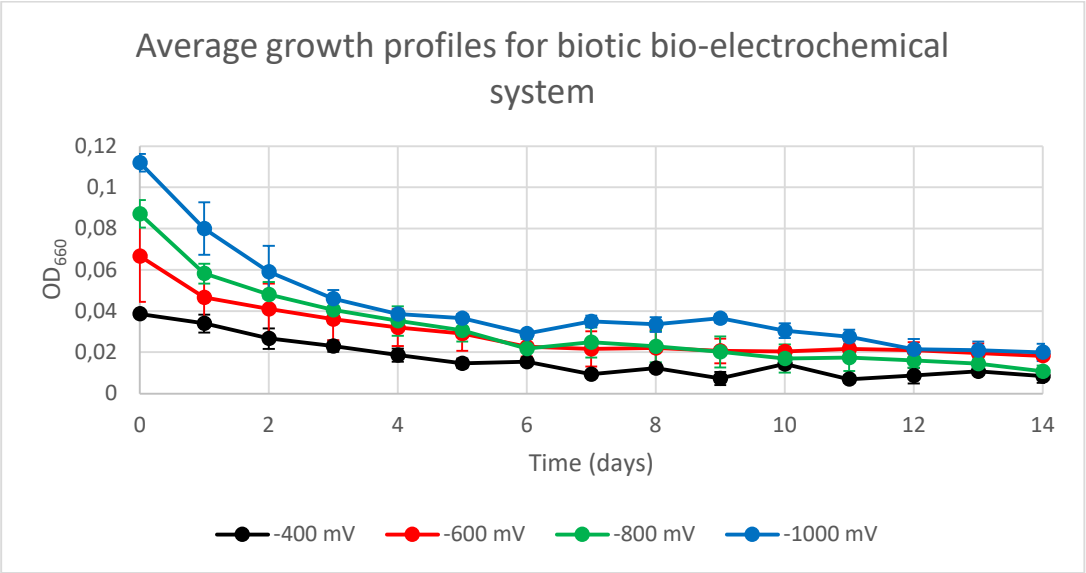

Figure A33. Average growth profiles for biotic bio-electrochemical system at the potentials -400, -600, -800 and -1000 mV, during a timespan of 14 days.

Appendix A4 – Average supplied charge for biotic and abiotic bio-electrochemical systems

Table A3. The average supplied charge for the biotic and abiotic bio-electrochemical system reactors at the potentials -400, -600, -800 and -1000 mV.

Potential (*mV*)	Biotic (*C*)	Abiotic (*C*)
-400	6165	9801
-600	253147	531337
-800	10318169	6334883
-1000	8127255	9153915